PVD and CVD gradient coatings on sintered carbides and sialon tool ceramics

L.A. Dobrzański, M. Staszuk*
Institute of Engineering Materials and Biomaterials, Silesian University of Technology, ul. Konarskiego 18a, 44-100 Gliwice, Poland
* Corresponding author: E-mail address: marcin.staszuk@polsl.pl

Abstract

Purpose: *The main objective of the work is to investigate the structure and properties of multilayer gradient coatings produced in PVD and CVD processes on sintered carbides and on sialon ceramics, and to define the influence of the properties of the coatings such as microhardness, adhesion, thickness and size of grains on the applicable properties of cutting edges covered by such coatings.*

Design/methodology/approach: *The investigation studies pertaining to the following have been carried out: the structures of the substrates and coatings with the application of transmission electron microscopy; the structure and topography of coating surfaces with the use of electron scanning microscopy; chemical composition of the coatings using the GDOES and EDS methods; phase composition of the coatings using X-ray diffraction and grazing incident X-ray diffraction technique (GIXRD); grain size of the investigated coatings using Scherrer's method; properties of the coatings including thickness, microhardness, adhesion and roughness; properties of the operating coatings in cutting trials. The models of artificial neural networks have been worked out which involve the dependencies between the durability of the cutting edge and properties of the coatings.*

Findings: *Good adhesion of the coatings to the substrate from sintered carbides is connected with the diffusive mixing of the components of the coating and substrate. In the case of PVD coatings obtained on sialon ceramics, the highest adhesion to the substrate (Lc=53-112 N) has been demonstrated by the coatings containing the AlN phase of the hexagonal lattice having the same type of atomic (covalence) bond in the coating as in the ceramic substrate. The damage mechanism of the investigated coatings depends to a high degree on their adhesion to the substrate. The durability of cutting edges covered by the investigated coatings depends principally on the adhesion of the coatings to the substrate, and to a lesser degree on the other properties.*

Practical implications: *While selecting a proper coating material on ceramic cutting edges, it is advisable to remember that the coatings having the same type of atomic bond as the ceramic substrate have higher adhesion to the substrate. Another relevant aspect of the research presented in the paper is the fact that the adhesion of the coatings contributes significantly to the durability of the cutting edge, whereas the microhardness of the coatings, their thickness and grain size have a slightly lower influence on the durability of the tool being coated.*

Originality/value: *The paper presents the research involving the PVD and CVD coatings obtained on an unconventional substrate such as sialon ceramics. Furthermore, to define the influence of coating properties on the durability of cutting edges, artificial neural networks have been applied.*

Keywords: *Working properties of materials and products, Mechanical properties, PVD and CVD coatings*

Reference to this paper should be given in the following way:

L.A. Dobrzański, M. Staszuk, PVD and CVD gradient coatings on sintered carbides and sialon tool ceramics, in L.A. Dobrzański (ed.) Effect of casting, plastic forming or surface technologies on the structure and properties of the selected engineering materials, Open Access Library, Volume 1, 2011, pp. 133-186.

1. Introduction

The process of machining at the beginning of the 21st century is still one of the most important production technologies applied in the industry of mechanical engineering. Even if we apply plastic hot or cold working or casting technologies, still the final working is most frequently done by machining [9,16,46,54,57,96].

The constantly improving properties of constructional materials, which are obtained through machining, are determining a demand for a high standard quality of produced tools which must satisfy such aspects as service life, hardness of the cutting edge as well as working conditions such as speed, depth and feed rate. It is the economic conditions which principally enforce the necessity to increase the efficiency of machining, which is being realized by raising the thickness of the material removed in a single pass and by reducing its time [10,42,49,70,73,84]. To meet such requirements, the tools should have high hardness and should be considerably resistant to abrasive, adhesive, diffusive and chemical wear [33,79].

Among a variety of tool making materials, sintered carbides are still a dominant group in view of machining technologies. Advantageous usability properties and hardness higher than that of high speed steel, and also a relatively low price involving their production costs make them popular and commonly applied. Furthermore, modern sintering methods make it possible to produce cutting edges from sintered carbides having very fine grains and properties better as compared to the carbides produced with standard methods [7,43,64,81]. On the other hand, the scientific and industrial environments are getting more and more interested in tool making ceramics, including also the β-sialon ceramics elaborated at the end of the 20th century. The mechanical properties of this alloy ceramics have been inherited from the isomorphic β-Si_3N_4, and the chemical properties correspond to aluminum oxide Al_2O_3 [56].

The hard coatings PVD and CVD used for cutting edges are an efficient means to increase the durability of tools made from high speed steel and sintered carbides, being already applied from the 1960s of the 20th century [4,63]. Recently, also the opinion stating that coating deposition on ceramic tools is aimless due to their hardness being high enough has been verified. There are ceramic tools offered recently on the market covered with coatings resistant to abrasion. The coatings resistant to wear based on nitrides, carbides, oxides and borides, principally of transition metals, make it possible to apply higher machining parameters of tools covered by them, and also enable working processes without the application of cutting-tool lubricants [11,12,22,23,25,72,85].

In spite of the fact that the coatings on machining cutting edges have been used for many years, their dynamic development can be observed during the last decade [4,16,18,23,25,28,29, 35,72]. At present, the modified PVD and CVD methods can be applied to produce coatings having extreme tribological properties of elements they are covered with. However, there is no universal coating which can have unlimited applicability. A wide range of coating applicability necessitates a proper selection of a coating depending on the actual application, deposition method and substrate type [68,78,88,96]. Presently we can distinguish two parallel research trends in the area of thin coatings. The first research trend is aiming to elaborate new coating types, possible search for new applicability for the already known coatings. The second research trend is connected with the development of deposition technologies of hard coatings resistant to wear, the search for new deposition methods and the modernization of the existing techniques [19,76].

The coatings resistant to wear are applied nowadays in all tool making materials, even the hardest ones [23,72]. The application of protective coatings has a considerable influence on the improvement of durability and efficiency of machining tools, due to the following factors [9]:

- high hardness of the operating surface of the tool covered with the coating; hardness is one of the basic qualities of surface layers; in most cases the rise of hardness results in the rise of the qualities of other coating systems [5,6].
- possibly low friction factor within the contact area between the tool and a machined object. This factor has a considerable influence on the machining process, among others through the reduction of machining forces, lowering the temperature; it also enables to do the machining without cutting tool lubricants, and it finally speeds up the machining process itself.
- creation of thermal barrier for the heat generated during the operation of the tool; lower temperature of the tool translates itself into lower thermal deformation, which contributes considerably to better durability of the tool [68].
- reduction in the diffusion of atoms in both directions along the path tool – machined object.

Thin coatings deposited with the PVD and CVD techniques on the cutting edges of machining tools are principally made up by nitrides, carbides, oxides, borides of transition metals (most frequently Ti, Zr, V, Cr, Mo, W, Nb, Hf) or their combinations. The interest aroused by these phases is connected with the fact that these hard-melting phases are usually very hard and brittle, and are usually resistant to corrosion and tribological wear [4,56,61,87].

The protective coatings can be divided into groups depending on the type of atomic bond dominating in a given type of coating. Having considered all types of coating materials, the most numerous group is made up by materials with the predominant number of metallic bonds. Here we can name such as nitrides and carbides of transition metals, but also some borides and silicides. In a great majority of these phases there are metallic-covalence bonds, whereby the said materials are combining in themselves high hardness and abrasive resistance with the resistance to brittle cracking, which is higher as compared to the phases of covalence and ionic bonds. Another group of coating materials is made up by materials with the prevalence of ionic groups. This group includes mainly oxides. And the third group is composed of materials with the prevalence of covalence bonds where we can place diamond coatings and those made from boron nitride. This group of materials has the highest hardness. Table 1 presents the examples of coatings from all three material groups [4,56].

The coatings from titanium nitride have been used since the 1960s of the 20th century and they are still widely applied in the industry [4,63], although we can observe a declining interest in this material in favor of other phases [3]. The titanium nitride crystallizes in a cubic lattice of NaCl type, and it is a typical interstitial phase of a very wide homogeneity range from 30 to 50% at. of nitrogen. The microhardness of this phase is growing proportionally with the

concentration of nitrogen (Table 1) [87]. The TiN layers have high resistance to abrasion [25,34,35,36], but they oxidize in the atmospheric air at the temperature of 670-870 K [3].

Table 1. *Selected properties of coating material about metallic, ionic and covalence bonds [4,56,66,96]*

Kind of bonding	Coating material	Microhardness, HV	Young's modulus, GPa	Density, g/cm^3	Coefficient of thermal expansion α, 10^{-6}·K
Metalic	TiN	2100-2400	256-590	5.40	9.35-10.1
	ZrN	1600-1900	510	7.32	7.9
	TiC	2800-3800	460-470	4.93	7.61-8.6
	ZrC	2600	355-400	6.63	6.93-7.4
	TiB_2	≥3000	560	4.50	7.8
Ionic	Al_2O_3	1800-2500	400	3.98	8.4-8.6
	TiO_2	1100	205	4.25	9.0
	ZrO_2	1200-1550	190	5.76	7.6-11.1
Covalent	C (diamond)	≥8000	910	3.52	1.0
	BN (cubic)	3000-5000	660	2.52	-
	BN (face centered)	4700	-	-	-
	AlN	1200	350	3.26	5.7

The admixture of other elements to the TiN phase such as zirconium, aluminum, carbon or boron results in the formation of isomorphic phases with titanium nitride [1,13,36,41,51,58,59,67, 77,82,90]. Multicomponent coatings Ti(C,N) are characterized by high hardness (2500-3500 HV0.05) [58] and by resistance to abrasion so they are applied for covering cutting tools from high speed steel and from sintered carbides [15,71,74,94]. In the coatings of (Ti,Al)N type, every second titanium atom is substituted with aluminum [59,77,82]. The presence of aluminum in such coatings results in the fact that the temperature of service durability of such coatings exceeds 970 K, and in working conditions with raised temperature a layer of Al_2O_3 is formed on the surface which generates a diffusion barrier for atmospheric oxygen [3,5,44,83]. By increasing the concentration of aluminum (Ti:Al 33:67) in (Al,Ti)N coatings we are raising the protective influence of this element [39]. The change of lattice parameters brought about by the dissolution of Al atoms in the TiN lattice is in congruence with the Vegard's law (Fig.1) [2,8]. We must note here that the metastable coatings (TiAl)N and (Al,Ti)N combine in themselves diverse properties of metallic-covalence materials (TiN) and of covalence ones (AlN) which can not be obtained as solid materials due to a different structure and a different type of bonds [96]. The coatings with the admixture of zirconium (Ti,Zr)N show better physical properties than TiN coatings, in particular hardness, resistance to

abrasion, wear and corrosion [90]. Such coatings can consist of single three-component phases and they can demonstrate two-component structure of TiN and ZrN [13,36,90]. In the case of Ti(B,N) coatings, their phase composition depends on the concentration of boron. Such coatings consist of single- or two-component phases, yet there are no three-component phases [41,47,48,60,66,67,95]. The microhardness of these coatings is within the range of 3000-5000 HV depending on phase composition. The highest hardness is demonstrated by Ti(B,N) coatings containing boron nitride [41,50]. Through the introduction of aluminum to the CrN coating, used as protective layers against corrosion and having good antiadhesive properties principally on plastic working tools, the nitride (Al,Cr)N was formed [37,40,61]. The admixture of aluminum of the concentration of 65-75% is stabilizing the AlN phase of the cubic lattice. Such coatings have high hardness and resistance to abrasion, higher than the conventional TiN coatings, whereby they can be applied to cover cutting edges. We should add here that such coatings exhibit high thermal stability, and their maximum operating temperature is 1100ºC [38,80].

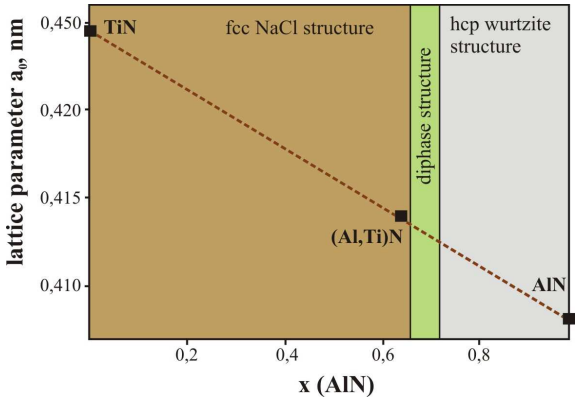

Figure 1. *Lattice parameters of the TiN, (Al,Ti)N films as a function of the AlN content and comparision with Vegard's law [2]*

Material designing is currently one of the most important issues of material engineering. A synergy obtained in the field of new material technologies involving the formation of structure and properties of surface layers of engineering materials has been brought about by the integration of many branches of science, engineering and technology. New materials and the technology of their manufacture is a challenge and great potential to be taken advantage of by the EU countries in view of hard competition with the developing countries of relatively cheap

workforce. The current approach to material designing is focused on the manufacture of materials having a structure ensuring that the materials have preset physicochemical properties meeting the specific requirements [30].

2. Materials

The research has been carried out on multi-point inserts from sintered carbides of the WC-Co type and from sialon tooling ceramics deposited and non-deposited with multilayer and gradient coatings resistant to abrasion in PVD and CVD processes. The inserts were being covered in the cathode arc evaporation process CAE-PVD with the coatings Ti(B,N), (Ti,Zr)N, Ti(C,N), Ti(C,N)+(Ti,Al)N, (Al,Ti)N, (Ti,Al)N and (Al,Cr)N, and in the high-temperature CVD process with multilayer coatings Ti(C,N)+Al_2O_3+TiN and Ti(C,N)+TiN.

3. Methodology

The surface topography and the structure of the produced coatings along the transverse fractures was observed on the scanning electron microscope Supra 35 of Zeiss Company. To obtain the images of the investigated samples, the detection of secondary electrons (SE) and backscattered electrons (BSE) was applied, with the accelerating voltage within the range of 5-20 kV.

The qualitative and quantitative analysis of the chemical composition in the microareas of the investigated coatings was carried out using the X-ray energy dispersive spectroscopy (EDS) with the application of the spectrometer EDS LINK ISIS of the Oxford Company being a component of the electron scanning microscope Zeiss Supra 35. The research was carried out with the accelerating voltage of 20 kV.

The orientation and grain size in the coating from sintered carbides was determined using the technique of Electron Backscatter Diffraction (EBSD) in the scanning electron microscope Supra 35 of Zeiss Company.

The changes of chemical concentration of the coating components along the direction perpendicular to its surface, and the concentration changes in the transit zone_between the coating and the substrate material were determined basing on the tests in the glow discharge optical spectrometer GDOS-750 QDP of the Leco Instruments Company. The following operating conditions of the Grimm tube of the spectrometer were applied: internal diameter of the tube 4 mm, voltage feed to the tube 700 V, tube current 20 mA, operating pressure 100 Pa.

The observation of the structure of thin foils and the diffraction research was carried out in the transmission electron microscope JEM 3010 UHL of the JEOL Company, with the accelerating voltage of 300 kV and maximum magnification of 25000 times. The diffractograms from the transmission electron microscope were solved with the use of the computer program "Eldyf".

The analysis of phase composition of the substrates and of the obtained coatings was carried out using the X-ray diffraction method (XRD) on the X-ray apparatus X'Pert of the Panalytical Company using the filtered radiation of a cobalt lamp. Due to the superposition of reflexes of the substrate material and coating and due to their intensity hindering the analysis of the obtained results, in order to obtain more accurate information from the surface layer of the investigated materials, we applied in our further investigation studies the grazing incident X-ray diffraction technique (SKP).

The assessment of grain size in the investigated coatings was carried out using the diffractograms obtained with the application of the grazing incident X-ray diffraction technique (SKP) using the Scherrer's method.

The measurement of roughness of the surface of the polished samples from sintered carbides of the WC-Co type and of sialon ceramics without coating and covered with the investigated coatings were carried out on the profilographometer Surtronic 3+ of Taylor Hobson Company, whereas the roughness measurement of the surface of gray cast iron after the technological machining trial with cutting edges without coatings and with the investigated coatings was carried out on the profilographometer Diavite Compact of Asmeo Ag Company. We assumed the measurement length of Lc=0.8 mm and measurement accuracy of ±0.02 μm. The parameter Ra acc. the Standard PN-EN ISO 4287:1999 was assumed as the quantity describing the roughness. We carried out 6 measurements on each of the investigated samples and we determined the average, standard deviation and confidence interval, assuming the confidence factor at $1-\alpha=0.95$.

The hardness of the investigated materials was determined using the Vickers method. The hardness of the covered substrates from sintered carbides and sialon tooling ceramics was determined making use of the classical Vickers method, using the loading equal to 3 N according to the Standard PN-EN ISO 6507-1:2007. The hardness measurement of the produced coatings was carried out using the dynamic method of Vickers, in the mode 'load-unload'.

Using the variance analysis for a single classification we assessed the statistical significance between many averages for hardness measurements. The following hypotheses were formulated:

H0: m1=m2=…=mt

versus an alternative hypothesis:

H1: the averages differ significantly.

The statistical significance between the particular averages was assessed basing on the variance relation between the averages in the separated groups and the overall variance of the investigated variable.

The adhesion of the coatings to the substrate was determined basing on the Scratch Test analysis on the apparatus Revetest of the CSEM Company. The critical load Lc at which the adhesion of the coating fails was determined basing on the value of acoustic emission recorded during the measurement and on the observation of scratches formed during the scratch test. The said observations were made on the light microscope being a component of the apparatus. Detailed observations of the formed damage were carried out on the scanning electron microscope DSM-940 of the Opton Company, with the accelerating voltage of 20 kV.

In order to categorize the investigated machining inserts according to their usability properties, technological machining trials were carried out. The tests involving the cutting ability of inserts from sintered carbides and sialon ceramics covered and non-covered with PVD and CVD coatings were carried out basing on cutting trials without cutting tool lubricants on the lathe TUR 630M. The machining at room temperature was applied on gray cast iron EN-GJL-250 of the hardness of about 215 HB. The durability of the investigated inserts was determined basing on the measurements of the width of wear band on the tool flank. The measurement of the average width of flank wear VB and of the maximum width of wear band VB_{max} was carried out using the light microscope Carl Zeiss Jena. The machining trials were being stopped when the assumed wear criterion for after-machining of VB=0.2 mm was exceeded. The observation of the wear of tool flank and attack surface of the machining inserts was carried out using the scanning electron microscope Zeiss Supra 35. The analysis of chemical composition in the microareas was carried out using the EDS method. The obtained results were presented in a graphical form as the relation of wear band on the tool flank VB in the function of cutting trial time. The durability of the cutting edge is defined as the time T [min] after which the value of the assumed criterion VB=0.2 mm is exceeded.

Basing on the set of experimental results, a model of artificial neural networks (SSN) was elaborated, which made it possible to determine if there is a dependency between the properties of the coatings such as microhardness, adhesion to substrate, grain size or coating thickness and the durability of cutting edges covered with the investigated coatings. We investigated the possibility to apply networks of different architecture such as: linear networks, radial base

functions (RBF), regressive networks (GRNN) and multilayer perceptron (MLP). From among the tested networks the best quality factors were obtained for the network of multilayer perceptron (MLP) with one hidden layer (Fig. 2).

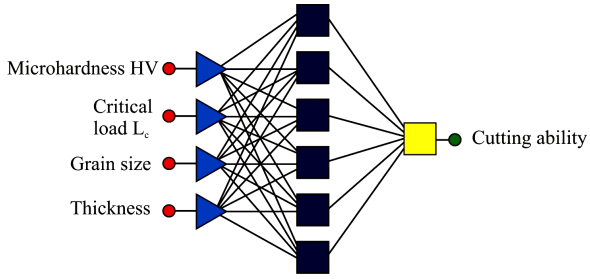

Figure 2. *Artificial neural network architecture of multilayer perceptron with one hidden layer*

The network was trained out using the algorithms of backward error propagation and coupled gradients. To verify the usefulness of the network we applied the average absolute error, standard deviation quotient and Pearson correlation factor.

4. Investigations results

Multi-point inserts from sintered carbides and from sialon tooling ceramics are characterized by well concentrated structure without pores or discontinuity (Fig. 3). The tests of thin foils in the electron transmission microscope have confirmed that the sintered carbides contain the grains of wolfram carbides WC of the hexagonal lattice (Fig. 4), and the sialons demonstrate isomorphic structure with silicon nitride Si_3N_4 of the hexagonal lattice. The phase composition of the investigated substrates was confirmed by the tests with the application of X-ray diffraction methods (Fig. 5).

In effect of the materialographic tests carried out on the scanning electron microscope it was found that the surface morphology of coatings produced with the PVD technique on sintered carbides of the WC-Co type and on tooling sialon ceramics is characterized by high non-homogeneity connected with the presence of numerous droplet-shaped microparticles (Figs. 6-9). The presence of these morphological defects is connected with the nature of cathode arc evaporation. The droplets observed in SEM are noticeably different in terms of size and shape. The size of these particles is within the range from the tenths of a micrometer to

around a dozen micrometers. Some particles have a regular shape, slightly flat, which can bespeak of high kinetic energy of the droplets colliding with a relatively cold substrate (Figs. 7, 9). We also observed solidified droplets of irregular shapes as well as agglomerates formed from several combined microparticles (Fig. 8). There were also some hollows formed probably when the solidified droplets break off after the PVD process has been completed (Figs. 7, 8). It was found that the hollows bespeaking of the breaking off of some microparticles frequently do not reach down to the substrate.

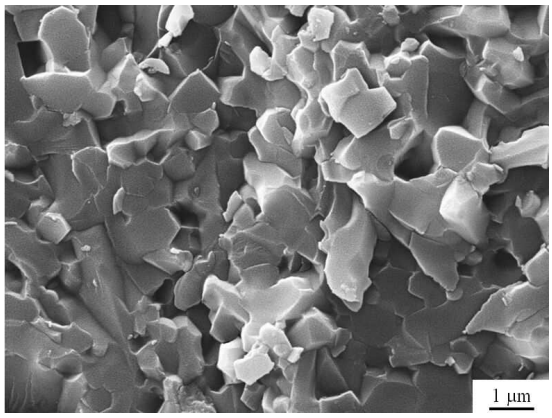

Figure 3. *Fracture of sialon tool ceramics*

The chemical analysis of particles present on the surface of PVD coatings (Fig. 9) shows that in these microareas there are predominantly metal elements from the evaporated shield pertaining to a given coating, i.e., titanium, zirconium and aluminum, which suggests that these are droplets of liquid metal broken off from the shield during the deposition of coatings and solidified on the substrate. In some cases the chemical analysis from the microarea of the droplet shows the presence of nitrogen, which can mean that a solidified metal droplet has been covered by a thin layer of coating material.

The analysis of surface morphology of coatings produced with the CVD technique on the substrate from sintered carbides and sialon ceramics shows that there occur networks of microcracks characteristic for this deposition method of thin coatings (Fig. 10). The surface of the coatings Ti(C,N)+Al_2O_3+TiN demonstrates a topography characteristic for the subsurface layer of Al_2O_3 consisting of numerous polyhedrons (Fig. 10). And the surfaces of the coating Ti(C,N)+TiN deposited on both substrates are different from each other. This coating deposited on sintered carbides has a slightly wavy surface of unsharpened shapes, and the coating Ti(C,N)+TiN on sialon consists of grains of spherical shapes and size of about 2 µm.

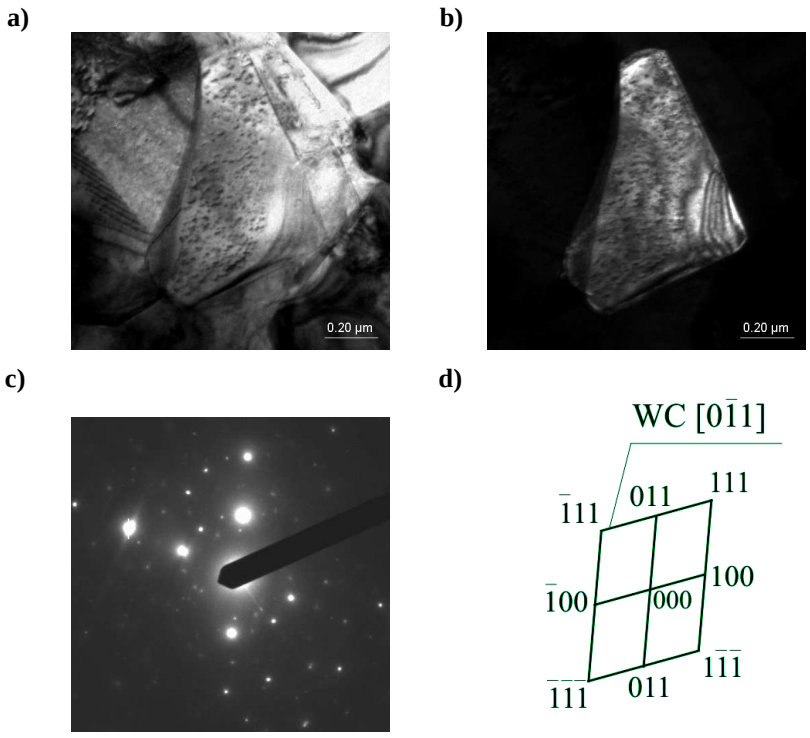

Figure 4. *Structure of sintered carbides substrate: a) bright field; b) dark field from 100 reflex; c) diffraction pattern from area b and d) solution of the diffraction pattern*

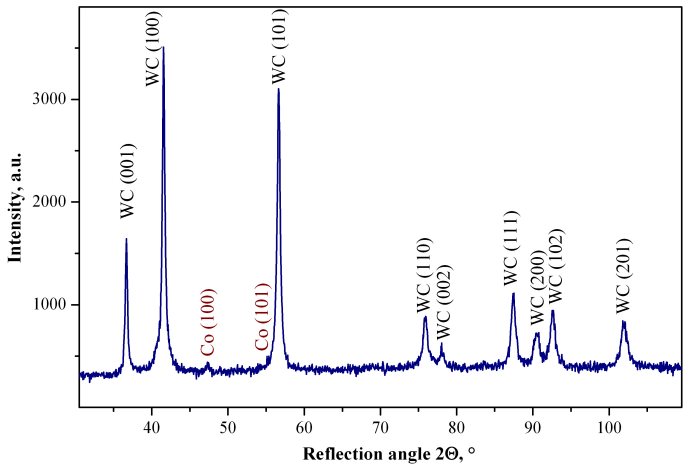

Figure 5. *X-ray diffraction pattern of sintered carbides substrate*

The morphology of coating surfaces has an influence on the rise of roughness Ra of the surfaces of inserts from sintered carbides and sialon ceramics covered by the investigated coatings (Table 2). The roughness of the multi-point inserts in both cases is the same and equals Ra=0.06 µm. The lowest rise of roughness of the surface is caused by the coating (Al,Ti) for which the averages Ra are 0.18 and 0.15 µm on the substrates respectively from sintered carbides and sialon ceramics. The highest roughness is demonstrated by the surfaces of samples covered by the CVD coating of the type Ti(C,N)+Al_2O_3+TiN, for which Ra is 0.63 µm in the case of sintered carbides and 0.82 µm in the case of sialons covered by the same coating. The roughness Ra of the surface of multi-point inserts covered by the PVD coatings is within the range from 0.15 to 0.50 µm, and the surface roughness with CVD coatings is within the range from 0.20 to 0.83 µm. However, there is no relation found between the durability of cutting edges and roughness of the coatings.

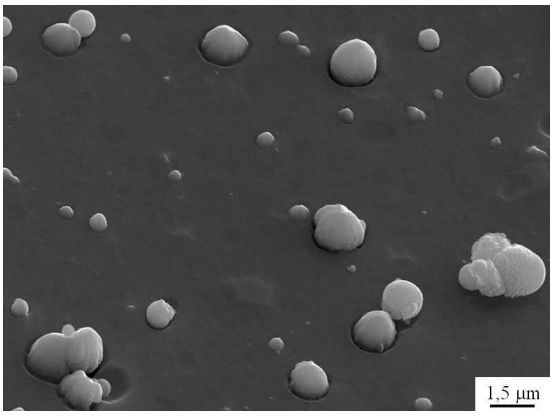

Figure 6. *Surface topography of the (Ti,Zr)N coating deposited onto the sintered carbides substrate*

Basing on the fractographic tests carried out in the scanning electron microscope, it was demonstrated that the PVD and CVD coatings are uniformly deposited and closely adhere to the substrate (Figs. 11-13). Furthermore, the particular layers of multilayer coatings Ti(C,N)+(Ti,Al)N, Ti(C,N)+Al_2O_3+TiN and Ti(C,N)+TiN are characterized by compact structure without delamination or defects and they closely adhere to one another (Fig. 13). It can be observed from the fractures of (Al,Cr)N coatings that this coating is also multilayer (Fig. 12), typical for multi-component coatings obtained through the application of separate sources of metal pairs Cr and Al. It was found that multilayer coatings of the type

Ti(C,N)+Al_2O_3+TiN and Ti(C,N)+TiN obtained by CVD method have a thin layer of fine-grained phase TiC in the interphase zone coating-substrate (Fig. 13), which was confirmed by X-ray diffraction methods and described in the further part of the paper. In addition, the Ti(C,N) layer in both CVD coatings is characterized by the structure which is changing in the gradient way from fine-grain close to the substrate and then turning gradually into column structure (Fig. 13). And the Al_2O_3 layer has the structure similar to the column one (Fig. 13).

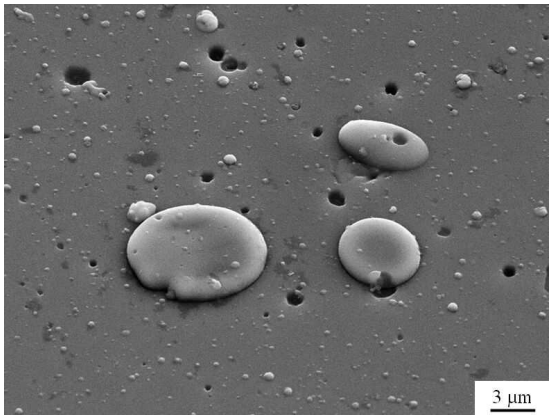

Figure 7. *Surface topography of the Ti(B,N) coating deposited onto the sialon ceramics substrate*

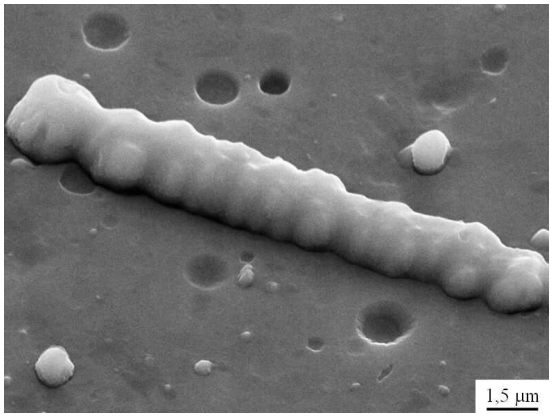

Figure 8. *Surface topography of the Ti(C,N) (2) coating deposited onto the sialon ceramics substrate*

The research on thin foils from Ti(B,N) coating deposited on the substrate from sintered carbides and sialon tooling ceramics confirms that in congruence with the assumptions the produced coatings contain phases of TiN type of the cubic lattice belonging to the spatial group Fm3m (Fig. 14). We must note here that due to the isomorphism of phases TiN and Ti(B,N) their diffractive differentiation is impossible. Also basing on the research on thin foils from the (Al,Ti)N coating it was demonstrated that this coating does not contain the AlN phase of the hexagonal lattice (spatial group $P6_3mc$) (Fig. 15) and TiN. All the observed structures of the coatings have high fine-grained character.

Table 2. *Roughness of investigated samples*

Coating	Roughness R_a, µm	
	Sintered carbides substrate	Sialon ceramics substrate
uncoated	0.06	0.06
Ti(B,N)	0.29	0.25
(Ti,Zr)N	0.30	0.40
Ti(C,N) (1)	0.22	0.23
Ti(C,N)+(Ti,Al)N	0.31	0.30
Ti(C,N) (2)	0.50	0.38
(Al,Ti)N	0.18	0.15
(Ti,Al)N	0.39	0.28
(Al,Cr)N	0.28	0.31
Ti(C,N)+Al_2O_3+TiN	0.63	0.82
Ti(C,N)+TiN	0.40	0.20

Table 3. *The results of quantitative chemical analysis from both X1 and X2 areas of coating Ti(C,N)+Al_2O_3+TiN deposited onto substrate from sintered carbides*

Element	Element of concentration, wt.%
C	15.20
N	10.93
Ti	73.87
O	41.50
Al	58.50

Also titanium droplets were found inside the investigated coatings whose presence is effected by the character of cathode arc evaporation. We also found the phases produced as a result of the solidification a droplet of the evaporated shield, which, due to the isomorphism of phases ε-TiN of the tetragonal latice and TiB of the rhombus lattice could not be explicitly identified (Fig. 16).

In effect of the qualitative X-ray microanalysis we obtained information about the elements present in the selected microareas of the investigated coatings (Figs. 9, 17), and in effect of the

quantitative analysis we obtained information about mass and atomic concentration of particular elements (Table 3). The qualitative and quantitative analysis EDS from the microareas of the coating demonstrates that the investigated layers contain elements appropriate for a given coating, and their quantitative composition is close to equilibrium. Additionally, in some cases the EDS spectrum shows the reflexes of the elements present in the substrate, and in the case of thin multilayer coatings the recorded result is an average of several layers whereof a given coating is composed. In the case of CVD coating of the type Ti(C,N)+Al_2O_3+TiN the analysis of chemical composition along the cross-section shows that the chemical composition of particular layers is close to equilibrium (Fig. 17, Table 3).

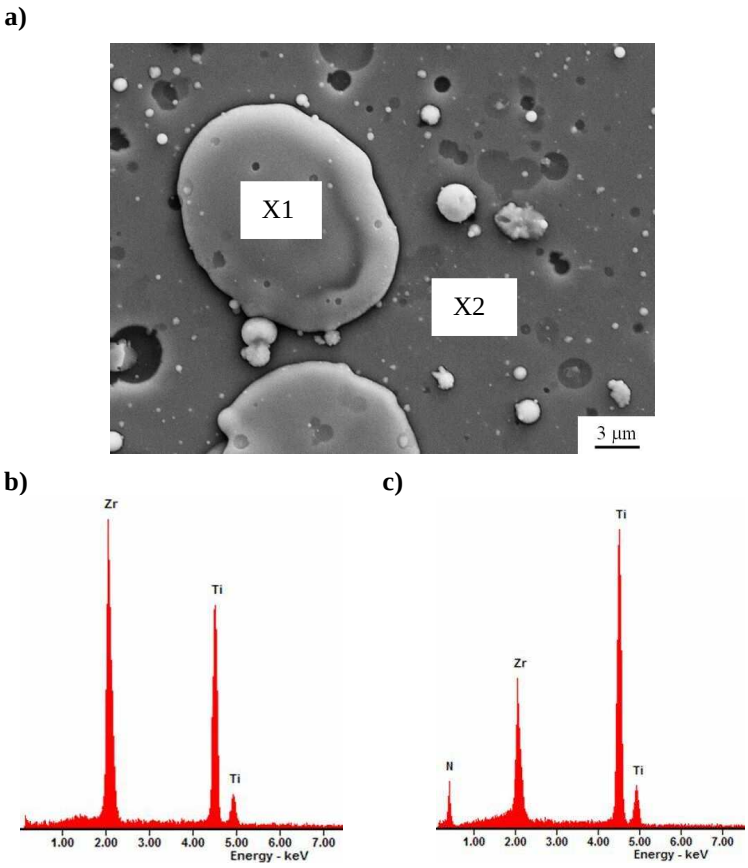

Figure 9. *Surface topography of the (Ti,Zr)N coating deposited onto the sialon ceramics substrate, b) X-ray energy dispersive plot the area X1 as in a figure a, c) X-ray energy dispersive plot the area X2 as in a figure a*

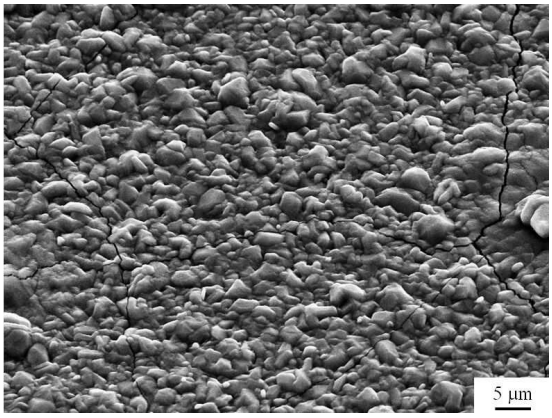

Figure 10. *Surface topography of the Ti(C,N)+Al_2O_3+TiN coating deposited onto the sialon ceramics substrate*

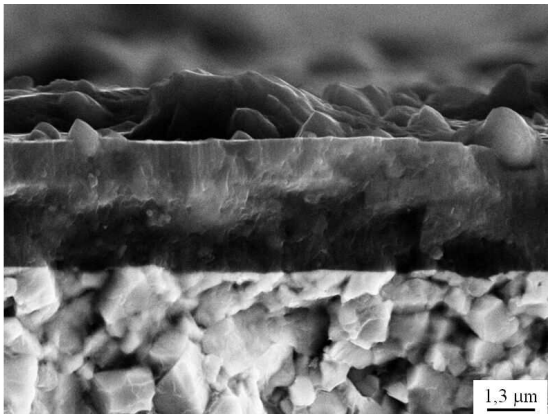

Figure 11. *Fracture of the Ti(C,N)+(Ti,Al)N coating deposited onto the sintered carbides substrate*

The research on chemical composition carried out on the glow discharge optical spectrometer GDOES confirms the presence of appropriate elements in gradient layers Ti(B,N), (Ti,Zr)N, Ti(C,N) (1), Ti(C,N) (2), (Al,Ti)N and in multilayer coatings Ti(C,N)+(Ti,Al)N, Ti(C,N)+TiN. Figures 18 and 19 present the changes of atomic concentration of the components of the coatings and of substrate material. The character of the changes of the concentration of elements which form the coatings bespeaks of their gradient structure. The character involving the concentration changes of the components in multilayer coatings of the type Ti(C,N)+(Ti,Al)N and Ti(V,N)+TiN is indicative of their multilayer

structure. In both cases, in the internal layer there occurs titanium, nitrogen and carbon, and in the external layer, respectively titanium, aluminum and nitrogen. In effect of the GDOES analysis it was demonstrated that in the contact zone from the surface of the coatings there is a concentration rise of elements that are components of the substrate with simultaneous decrease of the concentration of elements which are components of the coating. This fact can be caused by the presence of a transit zone of diffusive character between the substrate material and the coating, as it was suggested by the authors of earlier works [1,42,73,75], although we can not rule out the possibility of simultaneous non-homogeneous evaporation of the material from the surface of the samples during the tests on the glow discharge spectrometer.

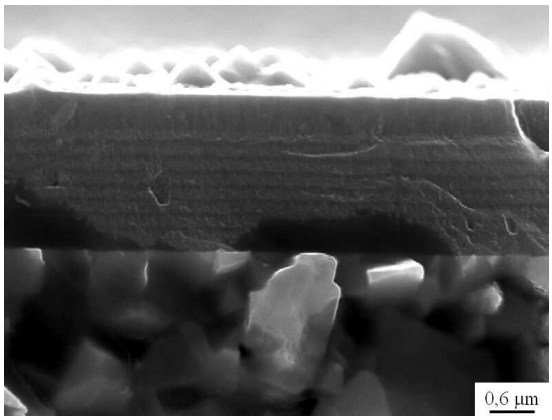

Figure 12. *Fracture of the (Al,Cr)N coating deposited onto the sintered carbides substrate*

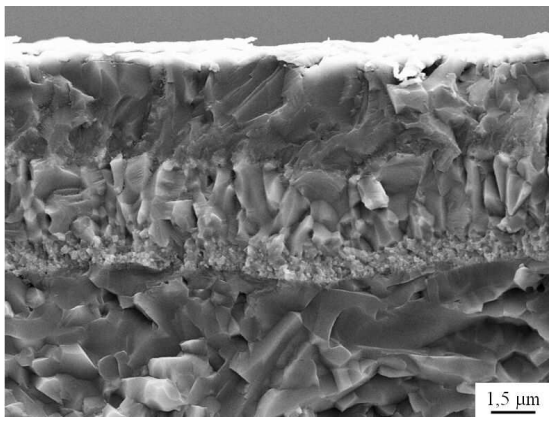

Figure 13. *Fracture of the Ti(C,N)+Al_2O_3+TiN coating deposited onto the sialon ceramics substrate*

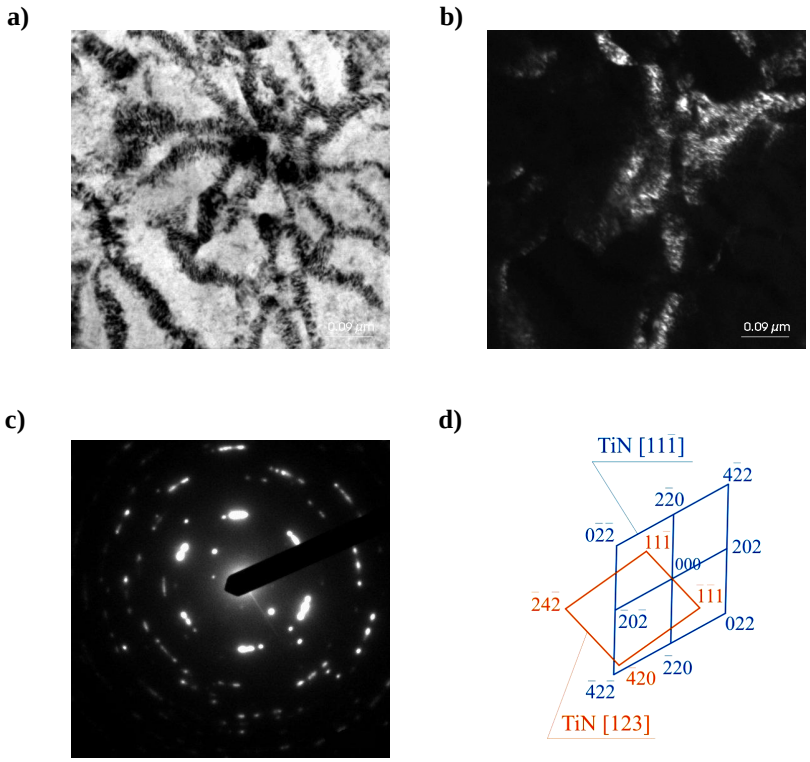

Figure 14. *Structure of Ti(B,N) coating: a) bright field; b) dark field from 0-2-2 reflex; c) diffraction pattern from area b and d) solution of the diffraction pattern*

The qualitative analysis of phase composition carried out with the X-ray diffraction method confirms that on the substrates from sintered carbides and sialon tooling ceramics, the coatings containing phases TiN, Ti(C,N), AlN and CrN were generated in congruence with the assumptions, and in the case of CVD coating - the phase Al_2O_3 (Figs. 20-23). On the X-ray diffractograms obtained with the use of Bragg-Brentano technique also the presence of the reflexes from phases WC and Si_3N_4 present in the substrate materials was demonstrated. The presence of reflexes from the substrate was found on all diffractograms from PVD coatings as well as on the diffractogram from the CVD coating of the type Ti(C,N)+TiN obtained on sialon ceramics, which is caused by the thickness of the obtained coatings 1.3-5.0µm, lower than the penetration depth of X-rays into the material. In effect of the tests with the application of grazing incident X-ray diffraction technique, at low incidence angles of the prime X-ray beam, we recorded the reflexes only from thin surface layers (Figs. 20b, 21b, 22b, 23a-c).

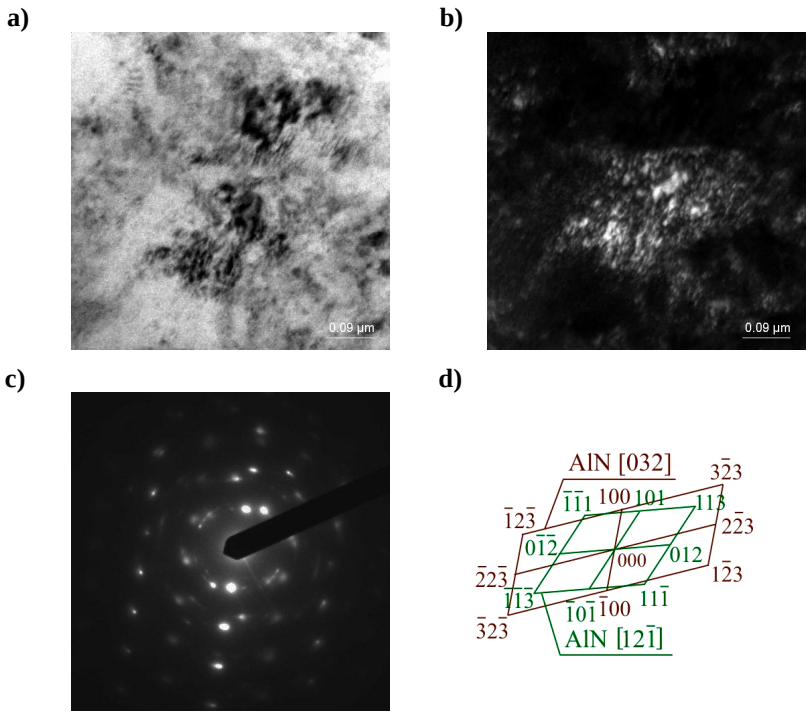

Figure 15*. Structure of (Al,Ti)N coating: a) bright field; b) dark field from -100 reflex; c) diffraction pattern from area b and d) solution of the diffraction pattern*

The lack of reflexes from the phases present in the substrates on the X-ray diffraction pattern obtained with the GIXRD technique bespeaks of the fact that the X-ray beam penetrating the investigated coatings did not get deep enough into the substrate. Table 4 presents the data involving the absorption depth of X-ray radiation depending on the incidence angle of the prime beam and on the type of chemical elements forming the coating material. Basing on the estimated absorption depths of X-rays and on the obtained diffraction patterns (Fig. 23a-c) we defined the structural models of multilayer coatings (Fig. 23d). It was demonstrated that the multilayer coatings Ti(C,N)+(Ti,Al)N, Ti(C,N)+Al_2O_3+TiN and Ti(C,N)+TiN contain appropriate phases for each of coating types in agreement with the assumed arrangement order of these phases. On the X-ray diffraction pattern obtained from the coatings Ti(B,N), (Ti,Zr)N, Ti(C,N)+(Ti,Al)N and (Ti,Al)N we found isomorphic phases from TiN, since these phases are a secondary solid solution on the basis of TiN. With respect to the coatings Ti(C,N) (1) and Ti(C,N) (2) the presence of titanium carbonitride was confirmed, and with respect to the coatings (Al,Ti)N and (Al,Cr)N the diffraction analysis confirmed the

presence of AlN phase of the hexagonal lattice in both coatings and of phases TiN and CrN respectively.

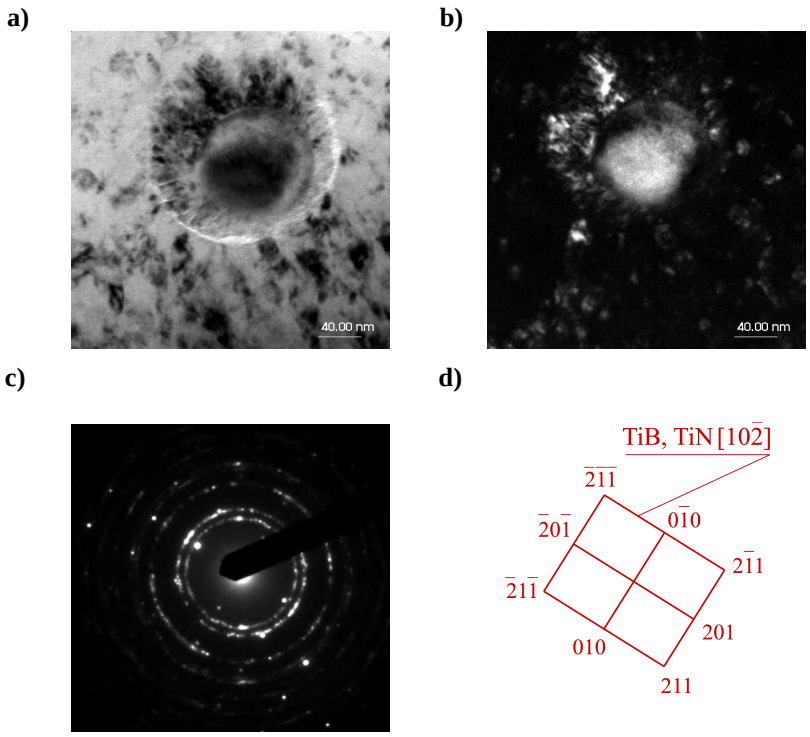

Figure 16. *Structure of Ti(B,N) coating: a) bright field; b) dark field from -20-1 reflex; c) diffraction pattern from area b and d) solution of the diffraction pattern*

Figures 24 and 25 present the assessment results of grain size from the coatings PVD and CVD obtained on the substrates from sintered carbides and sialon tooling ceramics. The data involving the grain size for the coatings obtained with PVD and CVD techniques is presented on separate diagrams due to considerably high differences of grain size for the coatings produced with these two techniques whereas the overall results of the carried out studies are presented in Table 5. The results show that the smallest grains are characteristic of the coating (Al,Ti)N in which the grain size values are 9.8 and 8.2 nm respectively for the coating obtained on the substrates from sintered carbides and sialon ceramics. The grain size of PVD coatings is within the range of 8.2-57 nm, and the grain size of the coatings obtained with the CVD technique is within the range of 112-421 nm. The measurement of the grain size shows that the coatings Ti(B,N), Ti(C,N) (1), Ti(C,N) (2), Ti(C,N)+(Ti,Al)N and (Ti,Al)N obtained on the

substrate from sintered carbides are characterized by smaller grains than the coatings of the same type obtained on sialon ceramics. In the case of coatings (Ti,Zr)N, (Al,Ti)N and (Al,Cr)N smaller grains are characteristic of the coatings obtained on sialon tooling ceramics. In general, the grain size range for the PVD coatings obtained on sialon ceramics is from 8.2 to 57 nm and is higher than the grain size range of the coatings obtained on the substrate from sintered carbides from 9.8 to 27 nm. A higher range is more advantageous for the analysis involving the influence of coating properties on cutting edge durability described in the further part of the work.

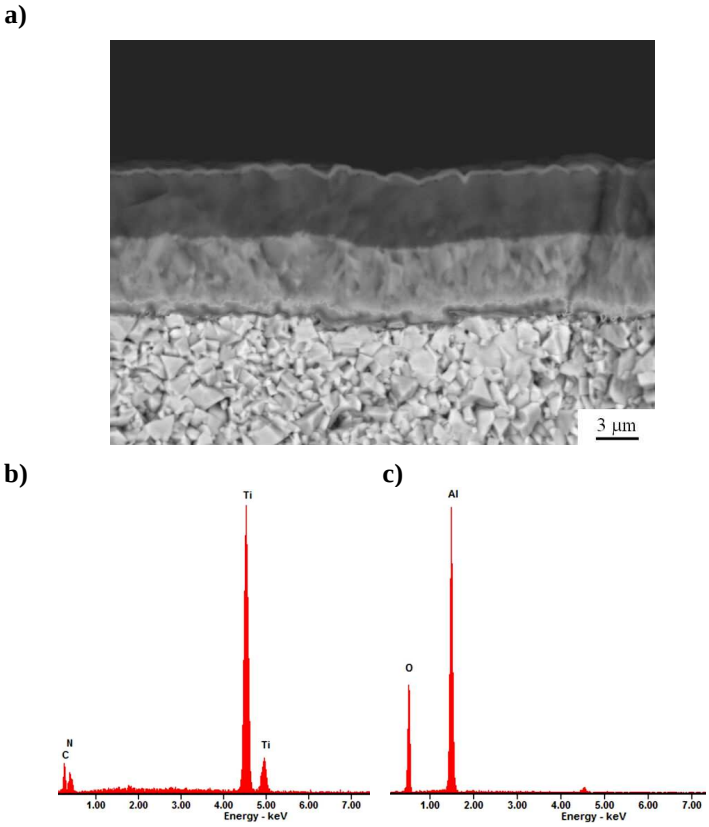

Figure 17. *Surface topography of the Ti(C,N)+Al_2O_3+TiN coating deposited onto the sintered carbides substrate, b) X-ray energy dispersive plot the area X1 as in a figure a, c) X-ray energy dispersive plot the area X2 as in a figure a*

The results of thickness measurements of the investigated coatings are presented in Table 6 and on the diagram presented in Fig. 26. The thickness of the investigated PVD coatings

obtained on sintered carbides and on sialon tooling ceramics is within the range from 1.3 to 5.0 µm, and the thickness of CVD coatings is from 2.8 to 8.4 µm. In effect of the carried out research it was demonstrated that both PVD and CVD coatings on sintered carbides have higher thickness than the coatings of the same type on the substrate from sialon ceramics. In the case of PVD coatings, this fact is definitely indicative of the possibility of substrate polarization, since the accelerating voltage has the influence on faster growing rate of the coatings than in the case of non-polarized ceramic substrate. With respect to CVD coatings, however, the higher thickness of coatings obtained on the substrate from sintered carbides results from the fact that the carbon in layers Ti(C,N) of both produced CVD coatings is not only from the operating gas but also from the substrate. The coatings (Ti,Al)N and (Al,Cr)N are here an exception since they have higher thickness on the sialon substrate.

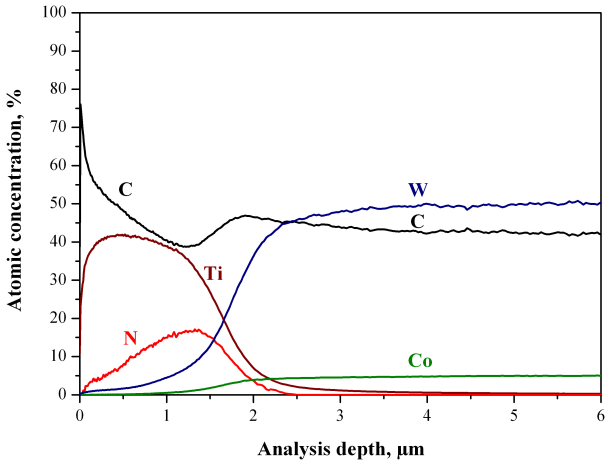

Figure 18. *Changes of constituent concentration of the Ti(C,N) (1) coating and the sintered carbides substrate material*

The research results involving the microhardness of sintered carbides and sialon ceramics without coatings and with the investigated coatings are presented in Table 7 and in Fig. 27. The analysis of statistical significance carried out for the coatings on the substrate from sintered carbides and sialon ceramics shows that there are significant differences between the average values of microhardness, so the zero hypothesis in both cases has been rejected (Table 8). In effect of the statistical significance test, three groups of microhardness have been singled out for each category i.e., for sintered carbides and sialon ceramics without coatings and for those covered by the investigated coatings (Tables 9, 10). The first group of the lowest

microhardness includes non-covered sintered carbides (Table 9) of the microhardness of 1826 HV 0.05, and in the case of sialon ceramics, sialons non-covered and covered with the coating (Al,Cr)N (Table 10) having average microhardness of 2132 HV0.05. And the microhardness of the substrate alone from the sialon ceramics is 2035 HV0.05 (Table 7, Fig. 27).

Table 4. *The depth of absorption X-ray radiation in a research coatings into diffraction analysis by GIXRD technique depending on incidence angle primary beam*

Coating	Sintered carbides substrate		Sialon ceramics substrate	
	α, °	τ, µm	α, °	τ, µm
Ti(B,N)	2	1.13	1	0.56
(Ti,Zr)N	2	1.25	2	1.25
Ti(C,N) (1)	2	1.14	2	1.14
Ti(C,N)+(Ti,Al)N	1	0.89	1	0.89
	2	1.40	2	1.40
	3	2.09	3	2.09
Ti(C,N) (2)	1	0.57	1	0.57
(Al,Ti)N	1	1.16	1	1.16
(Ti,Al)N	2	1.80	2	1.80
(Al,Cr)N	5	2.57	4	2.05
Ti(C,N)+Al_2O_3+TiN	0.5	0.28	0.5	0.28
	2	1.83	2	1.83
	5	5.16	4	4.13
Ti(C,N)+TiN	0.1	0.06	0.5	0.28
	1	0.57	3	1.71
	4	2.28	15	8.47

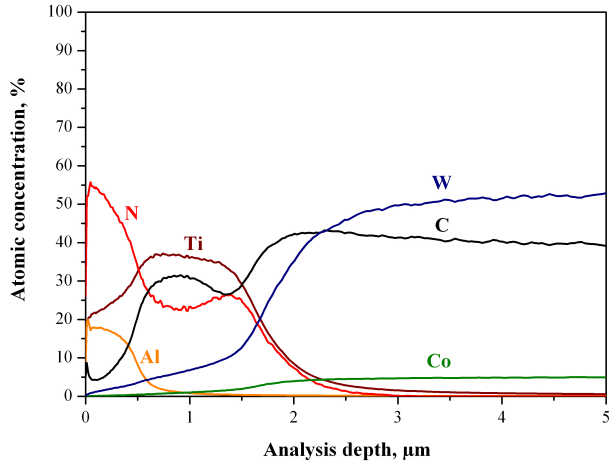

Figure 19. *Changes of constituent concentration of the Ti(C,N)+(Ti,Al)N coating and the sintered carbides substrate material*

The third group containing the coatings of the highest microhardness includes all PVD coatings obtained on the substrate from sintered carbides and the coating (Al,Ti)N obtained on sialon tooling ceramics, having the maximum value of microhardness equal to 3600 HV0.05. The microhardness of coatings obtained on sialon ceramics is within the range from 2230 to 3600 HV0.05, and the microhardness range of coatings on sintered carbides is lower and is within the range from 2315 to 2327 HV0.05.

a)

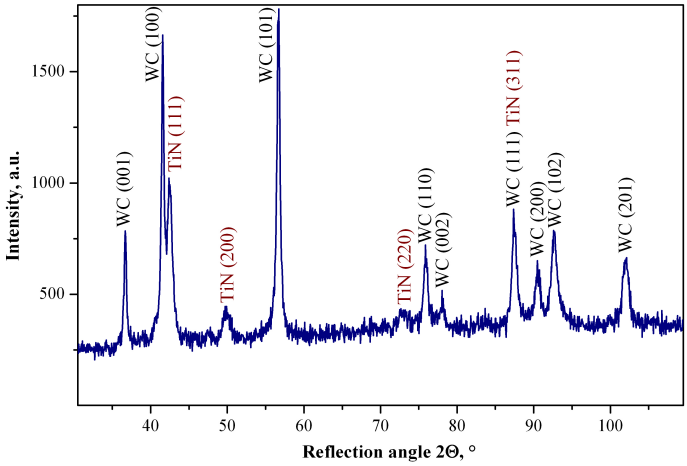

b)

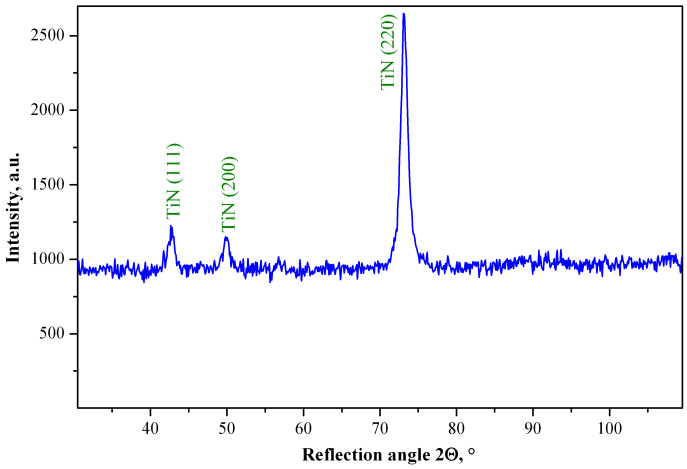

Figure 20. *X-ray diffraction pattern of Ti(B,N) coating deposited on the sintered carbides substrate obtained by: a) Bragg-Brentano method, b) GIXRD method (α=2º)*

a)

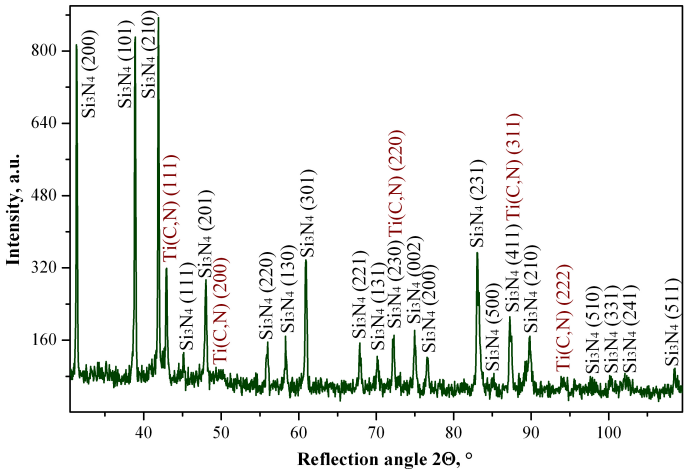

b)

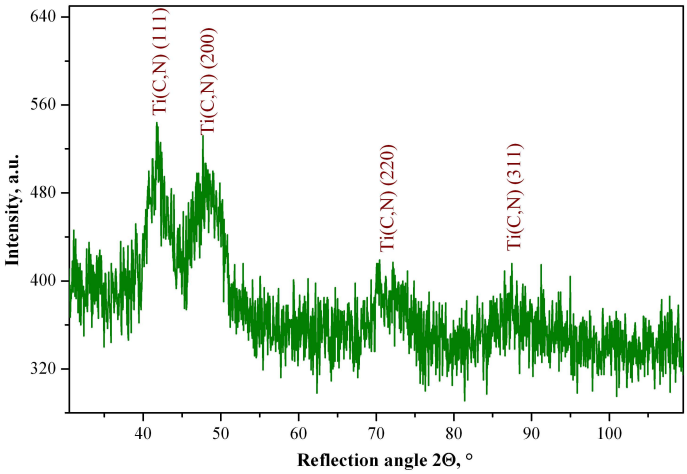

Figure 21. *X-ray diffraction pattern of Ti(C,N) coating deposited on the sialon ceraics substrate obtained by: a) Bragg-Brentano method, b) GIXRD method (α=1º)*

The critical load Lc [N] determined in the scratch test and being the measure of coating adhesion to the substrate considerably depends on the proper selection of coating material (chemical composition, phase composition) (Table 11, Figs. 28-32). This relation is particularly relevant with respect to PVD coatings on the substrate from sialon ceramics. The coatings in which only phases TiN and Ti(C,N) are present have low adhesion to the sialon substrate Lc=13-36 N, and the coatings containing the AlN phase are characterized by very

good adhesion to the substrate Lc=53-112 N. We must remember that sialons belong to covalence ceramics, and in the coatings containing isomorphic phases with titanium nitride TiN there are metallic bonds, which results in low adhesion of these coatings to the substrate of a different bond. In the case of coatings containing AlN phase of the hexagonal lattice there are covalence bonds analogous to the ceramic substrate, which yields good adhesion of these coatings to the substrate.

a)

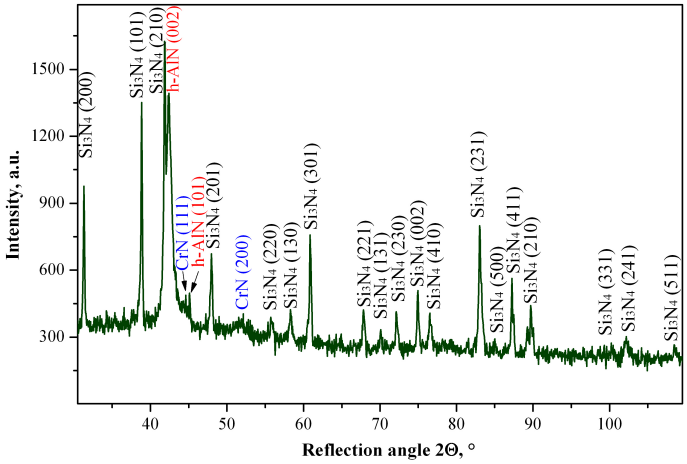

b)

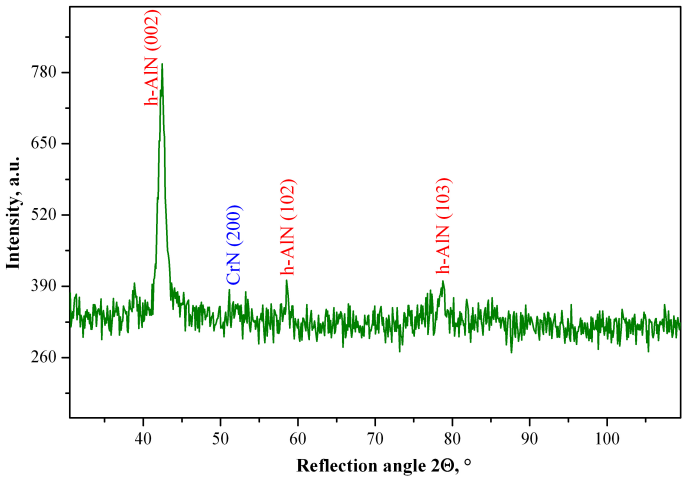

Figure 22. *X-ray diffraction pattern of (Al,Cr)N coating deposited on the sialon ceramics substrate obtained by: a) Bragg-Brentano method, b) GIXRD method (α=4°)*

a)

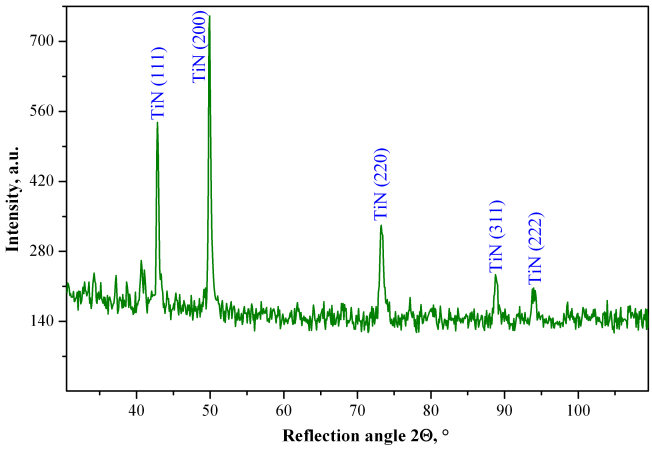
TiN (111)
TiN (200)
TiN (220)
TiN (311)
TiN (222)
Intensity, a.u.
Reflection angle 2Θ, °

b)

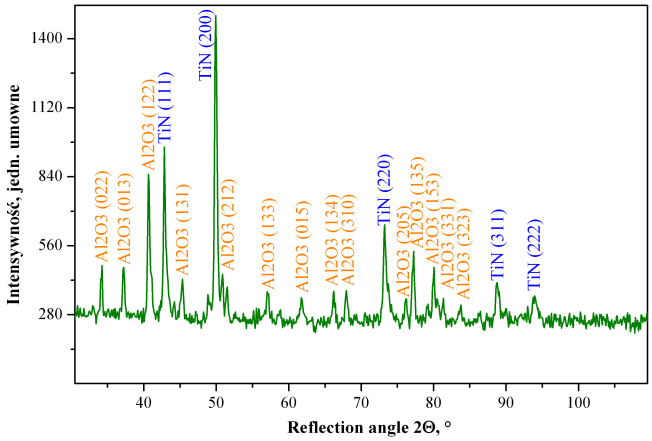
Al2O3 (022)
Al2O3 (013)
Al2O3 (122)
TiN (111)
Al2O3 (131)
TiN (200)
Al2O3 (212)
Al2O3 (133)
Al2O3 (015)
Al2O3 (134)
Al2O3 (310)
TiN (220)
Al2O3 (205)
Al2O3 (135)
Al2O3 (153)
Al2O3 (331)
Al2O3 (323)
TiN (311)
TiN (222)
Intensywność, jedn. umowne
Reflection angle 2Θ, °

c)

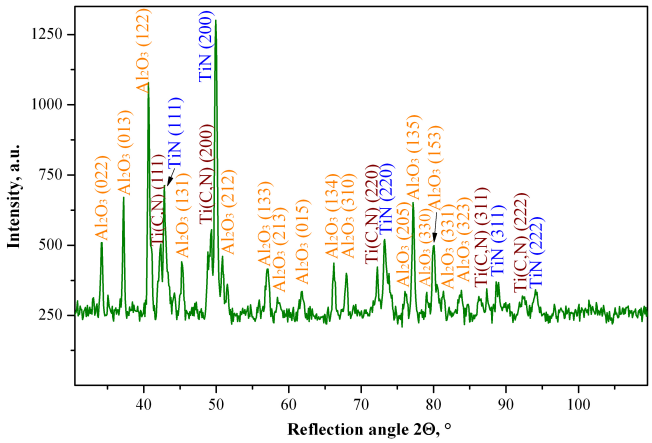
Al2O3 (022)
Al2O3 (013)
Al2O3 (122)
Ti(C,N) (111)
TiN (111)
Al2O3 (131)
Ti(C,N) (200)
TiN (200)
Al2O3 (212)
Al2O3 (133)
Al2O3 (213)
Al2O3 (015)
Al2O3 (134)
Al2O3 (310)
Ti(C,N) (220)
TiN (220)
Al2O3 (205)
Al2O3 (330)
Al2O3 (135)
Al2O3 (331)
Al2O3 (153)
Al2O3 (323)
Ti(C,N) (311)
TiN (311)
Ti(C,N) (222)
TiN (222)
Intensity, a.u.
Reflection angle 2Θ, °

d)

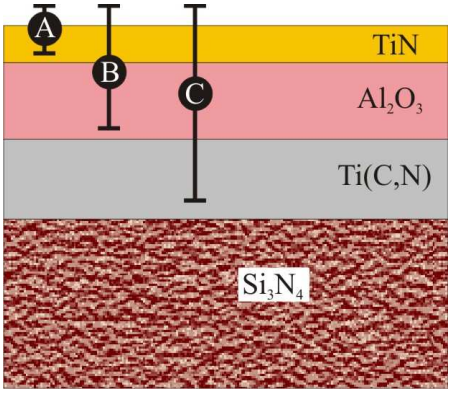

Figure 23. *X-ray diffraction pattern of Ti(C,N)+Al_2O_3+TiN coating deposited on the sialon ceramics substrate obtained by GIXRD method: a) α=0.5°, b) α=2 °, c) α=4°, d) Scheme of packing layers into Ti(C,N)+Al_2O_3+TiN coating, which was deposited on sialon tool ceramic with marking depths of GIXRD phase analysis: A for α=0,5°, B for α=2°, C for α=4°*

It means that the type of interatomic bonds present in the material of the substrate and coating has a great influence on the adhesion of coatings to the substrate. The adhesion of the coating to the substrate from sintered carbides is conditioned among others, apart from adhesion, by a slight diffusive displacement of elements in the contact zone, which is effected by the implantation of high energy ions falling down on the negatively polarized substrates.

Table 5. *Grain size in investigating coatings determined by Scherrer method*

Coating	Grain size, nm	
	Sintered carbides substrate	Sialon ceramics
Ti(B,N)	21	57
(Ti,Zr)N	21.4	13.6
Ti(C,N) (1)	17.7	21.3
Ti(C,N)+(Ti,Al)N	16.5	24
Ti(C,N) (2)	13.5	18.7
(Al,Ti)N	9.8	8.2
(Ti,Al)N	20.9	40
(Al,Cr)N	27.2	16.7
Ti(C,N)+Al_2O_3+TiN	250.7 [1)]	266.5 [1)]
	421 [2)]	324 [2)]
Ti(C,N)+TiN	356 [1)]	332 [1)]
	294.5 [3)]	112 [3)]

[1)] TiN layer; [2)] Al_2O_3 layer; [3)] Ti(C,N) layer

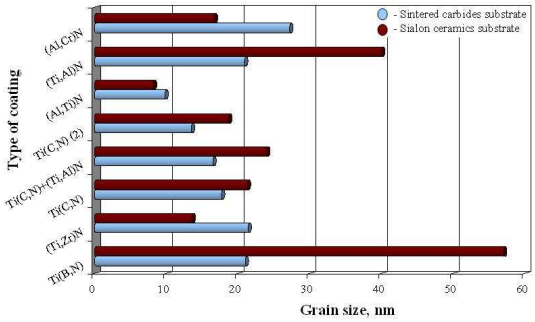

Figure 24. *The comparison of grain size PVD coatings on sintered carbides and sialon ceramics substrates*

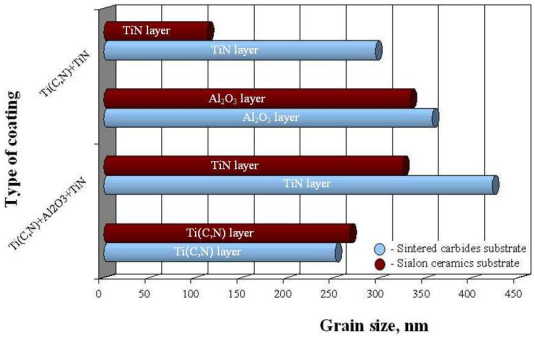

Figure 25. *The comparison of grain size CVD coatings on sintered carbides and sialon ceramics substrates*

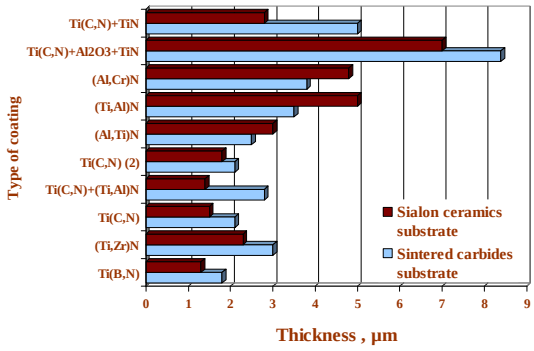

Figure 26. *The comparison of thickness coatings on sintered carbides and sialon ceramics substrates*

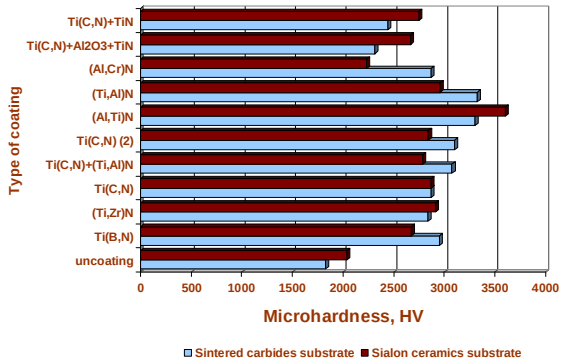

Figure 27. *The comparison of microhardness coatings on sintered carbides and sialon ceramics substrates*

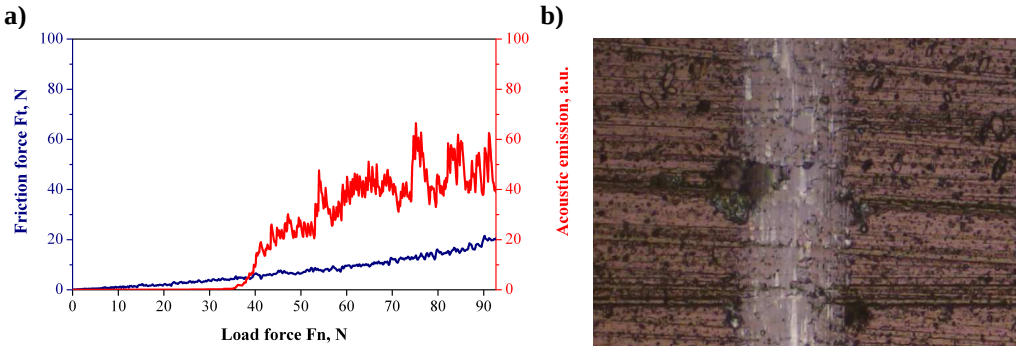

Figure 28. *a) Acoustic emission (AE) and friction force Ft as a function of the load Fn for Ti(C,N)+(Ti,Al)N coating on sintered carbides, b) scratch failure at L_c (opt) = 40 N, mag. 200 x*

Table 6. *Thickness of investigated coatings*

Coating	Thickness, µm	
	Sintered carbides substrate	Sialon ceramics substrate
Ti(B,N)	1.8	1.3
(Ti,Zr)N	3.0	2.3
Ti(C,N) (1)	2.1	1.5
Ti(C,N)+(Ti,Al)N	2.8	1.4
Ti(C,N) (2)	2.1	1.8
(Al,Ti)N	2.5	3.0
(Ti,Al)N	3.5	5.0
(Al,Cr)N	3.8	4.8
Ti(C,N)+Al_2O_3+TiN	8.4	7.0
Ti(C,N)+TiN	5.0	2.8

This has been demonstrated by the research results with the glow discharge optical spectrometer GDOES (Figs. 18 and 19), since, as described in the works [32,42,62], high energy ions falling down on the polarized substrate bring about various phenomena, among others local temperature rise, acceleration of chemisorption, intensification of surface diffusion and that into the substrate. Also a slight ion penetration might occur (about several nm down) as well as partial sputtering of atoms of the deposited coating.

Table 7. *The mean, standard deviation and confidence interval for 1-α=0.95 results of microhardness measurements of coatings deposited on sintered carbides and sialon tool ceramics as well as investigated surface materials*

Coating	Sintered carbides substrate			Sialon ceramics substrate		
	Microhardness, HV	Standard deviation	Confidence	Microhardness, HV	Standard deviation	Confidence
uncoated	1826	27	1804-1848	2035	32	2009-2060
Ti(B,N)	2951	158	2822-3080	2676	357	2386-2966
(Ti,Zr)N	2842	101	2759-2924	2916	393	2596-3235
Ti(C,N) (1)	2871	334	2599-3142	2872	365	2575-3269
Ti(C,N)+(Ti,Al)N	3076	432	2725-3426	2786	105	2700-2871
Ti(C,N) (2)	3101	270	2882-3321	2843	183	2694-2992
(Al,Ti)N	3301	370	3000-3602	3600	314	3345-3856
(Ti,Al)N	3327	494	2925-3729	2961	250	2758-3164
(Al,Cr)N	2867	502	2459-3275	2230	406	1900-2559
Ti(C,N)+Al_2O_3+TiN	2315	221	2135-2494	2669	315	2413-2926
Ti(C,N)+TiN	2443	205	2276-2610	2746	236	2554-2938

Table 8. *The variance analysis for mean microhardness results of coatings deposited on sintered carbides and sialon ceramic as well as investigated surface materials*

Sintered carbides substrate			Sialon ceramics substrate		
F	Value-p	Test F	F	Value-p	Test F
14.06	6.67^{-12}	2.01	11.31	3.34^{-10}	2.01

Table 9. *Results of significance test difference from division onto mean groups from microhardness measurements of coatings deposited on both sintered carbides and investigated substrate as well as results of the variance analysis for particular mean groups*

	Group 1	Group 2	Group 3
Coating	Sintered carbides uncoated	$Ti(C,N)+Al_2O_3+TiN$	Ti(B,N)
			(Ti,Zr)N
			Ti(C,N) (1)
			Ti(C,N)+(Ti,Al)N
		Ti(C,N)+TiN	Ti(C,N) (2)
			(Al,Ti)N
			(Ti,Al)N
			(Al,Cr)N
Average of group HV	1826	2379	3093
Analysis of variance			
F	-	1.89	1.08
Value-p		0.10	0.32
Test F		2.25	4.97

Table 10. *Results of significance test difference from division onto mean groups from microhardness measurements of coatings deposited on both sialon tool ceramics and investigated substrate as well as results of the variance analysis for particular mean groups*

	Group 1	Group 2	Group 3
Coating	Sialon ceramics uncoated	Ti(B,N)	(Al,Ti)N
		(Ti,Zr)N	
		Ti(C,N) (1)	
		Ti(C,N)+(Ti,Al)N	
	(Al,Cr)N	Ti(C,N) (2)	
		(Ti,Al)N	
		$Ti(C,N)+Al_2O_3+TiN$	
		Ti(C,N)+TiN	
Average of group HV	2132	2809	3600
Analysis of variance			
F	1.38	0.82	-
Value-p	0.27	0.57	
Test F	4.97	2.25	

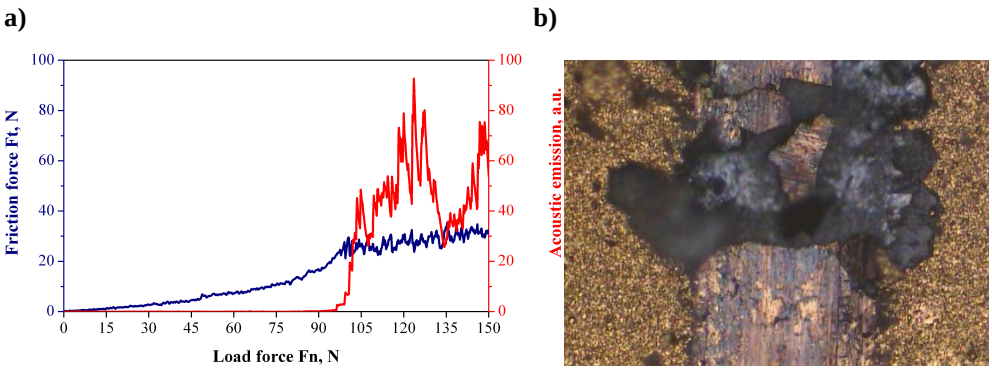

Figure 29. *a) Acoustic emission (AE) and friction force Ft as a function of the load Fn for Ti(C,N)+Al_2O_3+TiN coating on sintered carbides, b) scratch failure at L_c (opt) = 93 N, mag. 200 x*

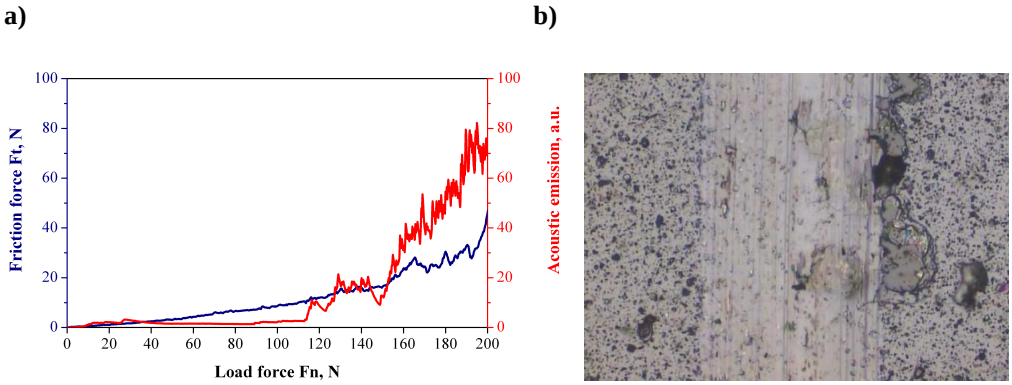

Figure 30. *a) Acoustic emission (AE) and friction force Ft as a function of the load Fn for (Al,Ti)N coating on sialon ceramics, b) scratch failure at L_c (opt) = 112 N, mag. 200 x*

The identification of defects of the coatings which occurred while doing the research on the adhesion with the scratch method was carried out through the observation in the scanning electron microscope and presented in Figs. 33-36. Furthermore, in order to investigate the produced defects more closely in some selected cases, when basing on the materialographic observations alone it was not possible to define if the produced defects penetrate into the substrate, the analysis of chemical composition in microareas was carried out using EDS, and we defined the surface distribution of chemical elements being in the coating and coming from

the substrate (Fig. 36). The research shows that there are four types of dominating damage mechanisms which are accompanied to a lesser degree by other phenomena. The first basic damage mechanism of coatings observed after exceeding the critical load is one-sided and two-sided delamination which principally involves the coatings obtained on the substrates from sintered carbides of the type Ti(B,N), (Ti,Zr)N, Ti(C,N)+(Ti,Al)N, (Al,Ti)N, Ti(C,N)+Al_2O_3+TiN and Ti(C,N)+TiN (Fig. 33), and also the coatings Ti(B,N), Ti(C,N) (1) and Ti(C,N) (2) obtained on sialon ceramics.

a) **b)**

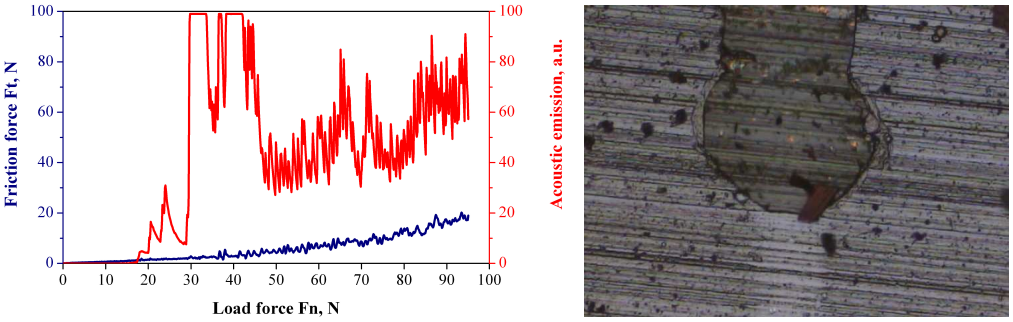

Figure 31. *a) Acoustic emission (AE) and friction force Ft as a function of the load Fn for (Ti,Al)N coating on sialon ceramics, b) scratch failure at L_c (opt) = 21 N, mag. 200 x*

Table 11. *The critical loads L_c of investigated coatings*

Coating	Critical load L_c, N	
	Sintered carbides substrate	Sialon ceramics substrate
Ti(B,N)	34	13
(Ti,Zr)N	40	21
Ti(C,N) (1)	49	25
Ti(C,N)+(Ti,Al)N	39	36
Ti(C,N) (2)	77	26
(Al,Ti)N	100	112
(Ti,Al)N	109	21
(Al,Cr)N	96	53
Ti(C,N)+Al_2O_3+TiN	93	43
Ti(C,N)+TiN	110	72

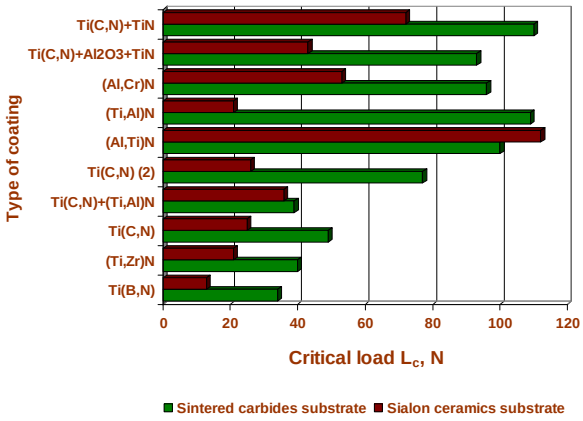

Figure 32. *The comparison of critical load L_c of coatings on sintered carbides and sialon ceramics substrates*

Table 12. *The results of tool life T measurements of investigated inserts*

Coating	Tool life T, min	
	Sintered carbides substrate	Sialon ceramics substrate
uncoated	2	11
Ti(B,N)	15	5
(Ti,Zr)N	13	5.5
Ti(C,N) (1)	13	5
Ti(C,N)+(Ti,Al)N	15	6
Ti(C,N) (2)	53	9
(Al,Ti)N	55	72
(Ti,Al)N	60	9
(Al,Cr)N	45	50
Ti(C,N)+Al_2O_3+TiN	23	3
Ti(C,N)+TiN	27	15

The second dominant damage mechanism is total delamination and it involves coatings of the type Ti(C,N) (1) and Ti(C,N) (2) obtained on the substrate from sintered carbides (Fig. 34). But initially, just after exceeding the critical load the two-sided delamination is taking place which, with increasing load, turns into total delamination. In addition, in all coatings obtained on the substrate from sintered carbides we found inside the scratch the defects effected by tension as well as chipping one- and two-sided along the borders of the scratch. Another damage mechanism found only in the case of coatings obtained on sialon ceramics of the type

(Ti,Zr)N, Ti(C,N)+(Ti,Al)N, (Al,Ti)N and Ti(C,N)+TiN is abrasion which was accompanied by cohesive fractures of the coatings and slight chipping and spalling (Fig. 35). It should be emphasized that in the case of coatings (Al,Ti)N and Ti(C,N)+TiN on the sialon substrate, even with maximum load, which is respectively 200 and 100 N, the coating was not ruptured but there were only a few cohesive defects and slight chipping. The fourth damage mechanism dominating in the coating Ti(C,N)+Al_2O_3+TiN obtained on the sialon ceramics involves vast chipping and spalling which occurred immediately after exceeding the critical load (Fig. 36).

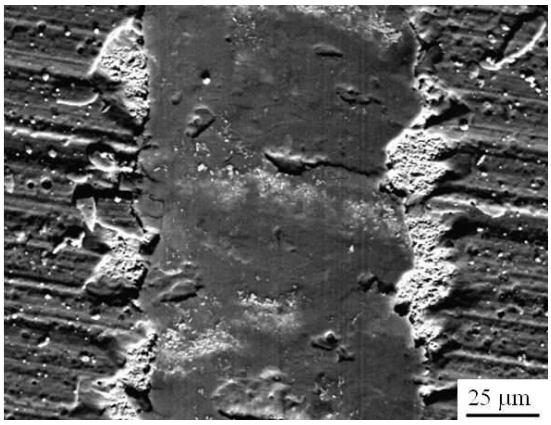

Figure 33. *Characteristic failure obtained by Scratch Test of the (Ti,Zr)N coating deposited on sintered carbides substrate*

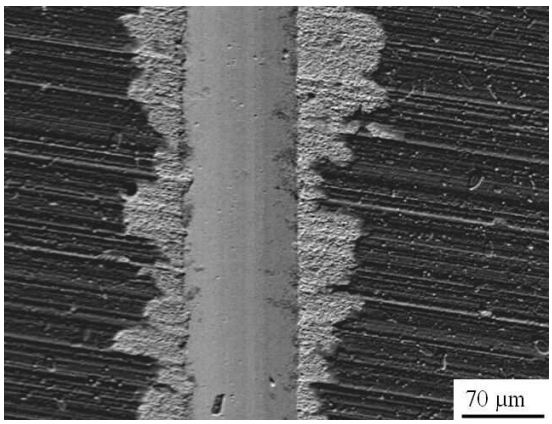

Figure 34. *Characteristic failure obtained by Scratch Test of the Ti(C,N) (1) coating deposited on sintered carbides substrate*

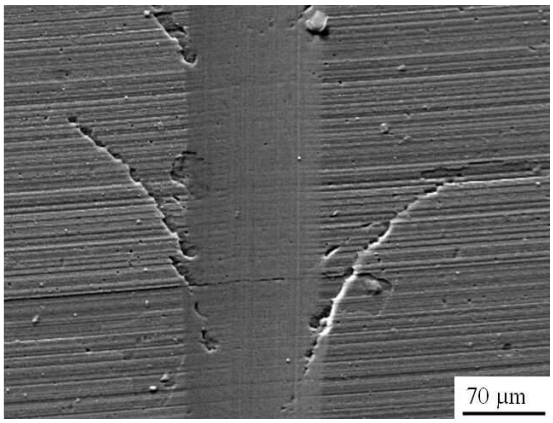

Figure 35. *Characteristic failure obtained by Scratch Test of the (Al,Ti)N coating deposited on sialon ceramics substrate*

The diagram involving the dependence of wear band VB on the tool flank on the machining time T is presented in Fig. 37, and the overall results are presented in Fig. 38 and Table 12. The research has a comparative character and its objective was to produce a durability ranking of coatings. It was found that the highest operating durability T=72 min of the inserts from sialon ceramics was obtained for the cutting edge covered by the (Al,Ti)N coating, and the lowest durability of the cutting edge T=5 min on the same substrate was exhibited by the coatings Ti(B,N) and Ti(C,N) (1).

The durability of the cutting edge from sialon ceramics without the coatings was estimated at T=11 min, which means that the coatings Al,Ti)N, (Al,Cr)N and Ti(C,N)+TiN have the influence on the rise of durability of the sialon cutting edge. In the case of inserts from sintered carbides, the highest influence on the durability of the cutting edge T=60 min has the (Ti,Al)N coating, and slightly lower T=55 and 53min the coatings (Al,Ti)N and Ti(C,N) (2) respectively. With respect to sintered carbides, all coatings increase the durability of the cutting edge since the durability of the non-covered tool is T=2 min, and the durability of the inserts of the lowest cutting ability with the coatings (Ti,Zr)N and Ti(C,N) (1) is T=13. Both in the case of covered sialon ceramics and covered sintered carbides a wide durability range of cutting edges was obtained depending on the type of deposited coating.

In effect of the materialographic observations of the investigated multi-point inserts in the scanning electron microscope it was demonstrated that the tools subjected to machining trials show their wear according to abrasive and adhesive mechanism (Figs. 39, 40).

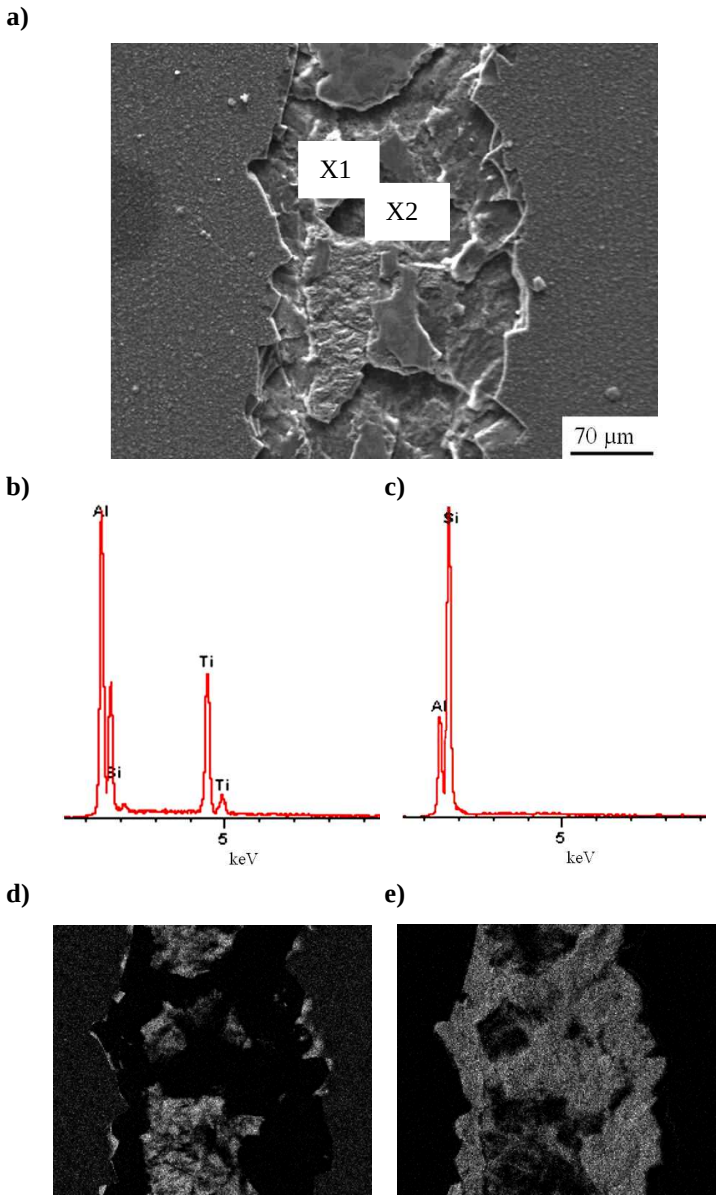

Figure 36. *a) Characteristic failure obtained by Scratch Test of the Ti(C,N)+Al_2O_3+TiN coating deposited on sialon ceramics substrate, b) X-ray energy dispersive plot the area X1 as in a figure a, c) X-ray energy dispersive plot the area X2 as in a figure a. Maps of superficial distribution chemical elements from areas as in a figure a: d) Ti - area with a coating, e) Si - area without a coating (images d and e were reduced)*

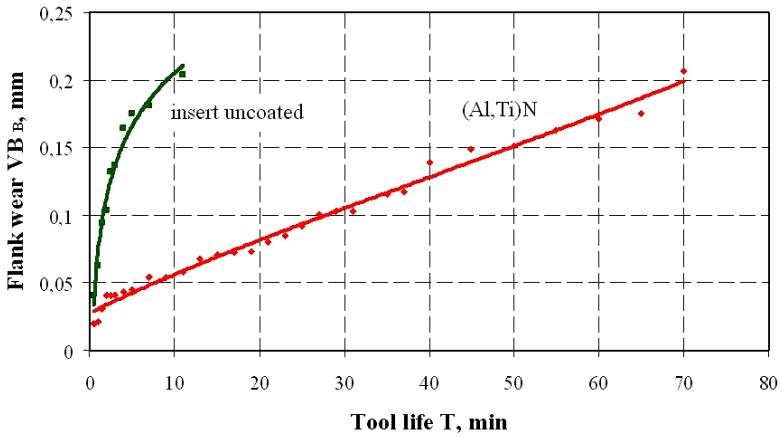

Figure 37. *Dependency graph the width of wear band on the tool flank on machining time T for sialon ceramic with deposited coating (Al,Ti)N*

On the tool flank, in particular on the cutting edges from sintered carbides with and without coatings, we found a build-up of the machined material, which is confirmed by the presence of iron reflexes on EDS graphs from the microareas (Figs. 39 b,c). We also found spalling of the coatings Ti(B,N), (Ti,Zr)N, Ti(C,N) (1), Ti(C,N)+(Ti,Al)N on the ceramic substrate and vast chipping of the coating Ti(C,N) (2) on the same substrate after 9 minutes of machining (Fig. 40).

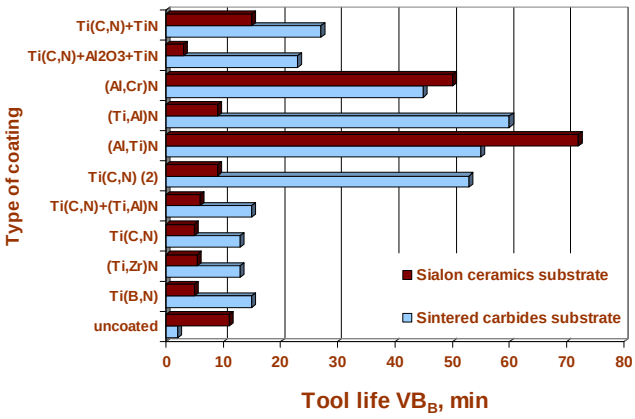

Figure 38. *The comparison of tool life T of investigated inserts*

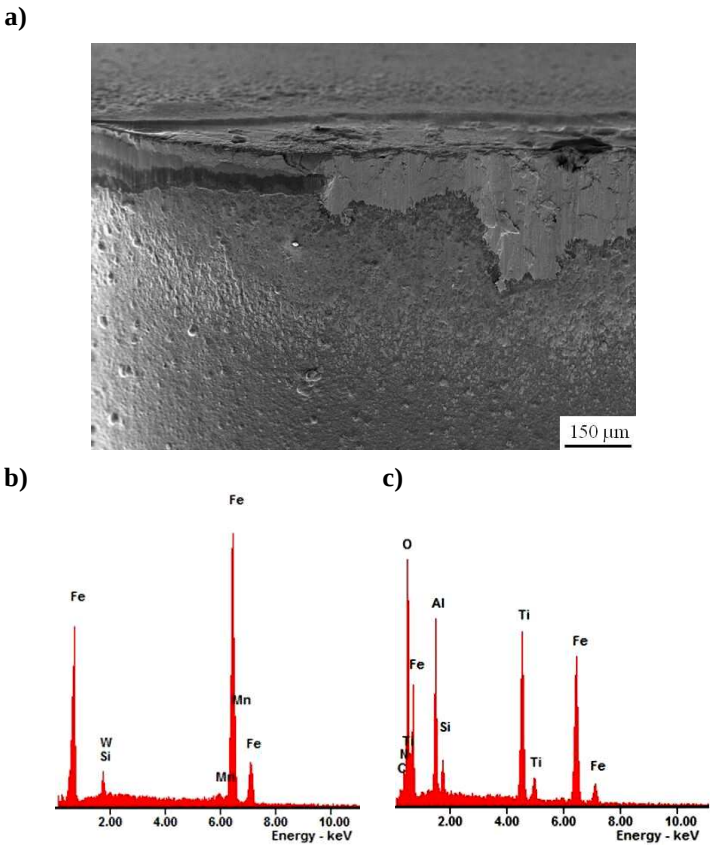

Figure 39. *a) Characteristic wear of tool flank of sintered carbides inserts with Ti(C,N)+Al_2O_3+TiN coating, b) X-ray energy dispersive plot the area X1 as in a figure a, c) X-ray energy dispersive plot the area X2 as in a figure a*

The surface quality of gray cast iron after machining with multi-point inserts without coatings and covered with the investigated coatings was determined on the basis of the measurement of the average deviation of roughness profile Ra of the machined surface (Table 13). The coatings bring about lower value of roughness Ra of the cast iron surface, and hence ensure better quality of the machined surface. The roughness Ra of the cast iron after the machining with cutting edges without coating is 4.55 µm in the case of inserts from sintered carbides and 3.03 µm in the case of sialons. We should emphasize here that the coating (Al,Cr)N leads to the quality deterioration of the gray cast iron surface yet the said differences, as it has been demonstrated by the statistical significance test, are irrelevant. Furthermore, the quality of the surface of gray cast iron after the machining with covered sialons is better than

after the machining with covered sintered carbides, and the average roughness difference is Ra=1.75 µm.

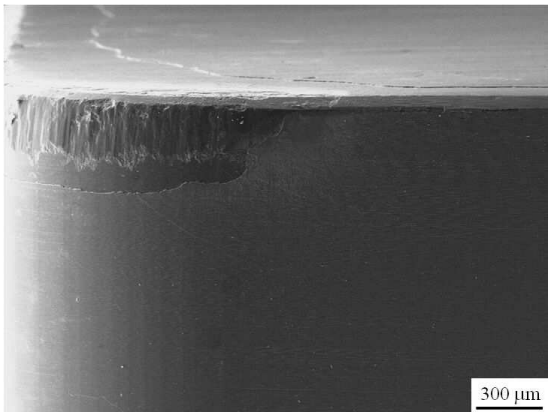

Figure 40. *Characteristic wear of tool flank of sialon tool ceramics inserts with (Ti,Al)N coating*

Table 13. *Roughness of gray cast iron after machining*

Coating	Roughness R_a, µm	
	Sintered carbides substrate	Sialon ceramics substrate
uncoated	4.55	3.03
Ti(B,N)	4.02	2.22
(Ti,Zr)N	3.82	1.96
Ti(C,N) (1)	4.51	2.06
Ti(C,N)+(Ti,Al)N	4.01	2.20
Ti(C,N) (2)	4.16	2.34
(Al,Ti)N	3.86	2.18
(Ti,Al)N	3.50	2.07
(Al,Cr)N	4.89	3.22
Ti(C,N)+Al_2O_3+TiN	3.69	2.76
Ti(C,N)+TiN	4.41	2.09

In the work we applied artificial neural networks to estimate the influence of the properties of the investigated coatings on the durability of cutting edges from sialon ceramics and sintered carbides covered by these coatings. The values of average absolute error, standard deviation and Pearson's correlation factor for the training, validating and testing sets presented in Table 14 bespeak of the fact that the applied artificial neural networks properly reproduce the

modeled relations. It follows from the sensitivity analysis of input data on output data (Table 15) that the durability of the cutting edge is principally influenced by the adhesion of the coatings to the substrate. The change of the critical load being the measure of coating adhesion has the highest influence on the change of cutting edge durability (Figs. 41, 42, 44).

Table 14. *Regression statistics of artificial neural network trained for prediction of PVD and CVD coatings properties deposited onto sialon ceramics*

Network architecture	Regression statistics	Data sets		
		Training Set	Validation Set	Testing Set
MLP3 4:4-6-1:1	Average absolute error	2.57	2.17	2.74
	Standard deviation ratio	0.14	0.10	0.19
	Pearson correlation	0.99	0.99	0.98

Table 15. *Results of sensitivity analysis of input data for output data of artificial neural network trained for prediction of PVD and CVD coatings properties deposited onto sintered carbides*

Data sets	Statistics	Microhardness	Critical load L_c	Grain size	Thickness
Training	Range	4	1	2	3
	Error	2.78	20.30	18.45	5.11
	Ratio	1.33	9.71	8.82	2.44
Validation	Range	4	1	2	3
	Error	3.08	27.12	15.26	4.89
	Ratio	2.49	21.96	12.36	3.96

The other properties such as microhardness, coating thickness and grain size have less significant influence on the changes of durability of the investigated cutting edges (Figs. 41-44). We must emphasize here that from among the other properties the grain size has the highest influence on the change of durability of the investigated cutting edges (Fig. 42), in particular in the case of covered sialon ceramics, yet the durability of the cutting edges is inversely proportional to the grain size. The change of microhardness and the thickness change of the investigated coatings only slightly influence the durability change of the investigated machining cutting edges.

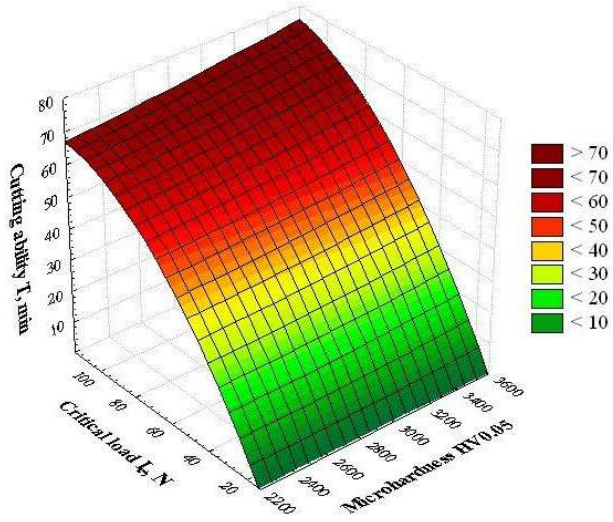

Figure 41. *Evaluation of the PVD and CVD coatings critical load and the microhardness influence of tool life T for sialon ceramics tools coated with PVD and CVD coatings determined by artificial neural networks at a fixed coating thickness 3.0 microns and particle size 8.2 nm*

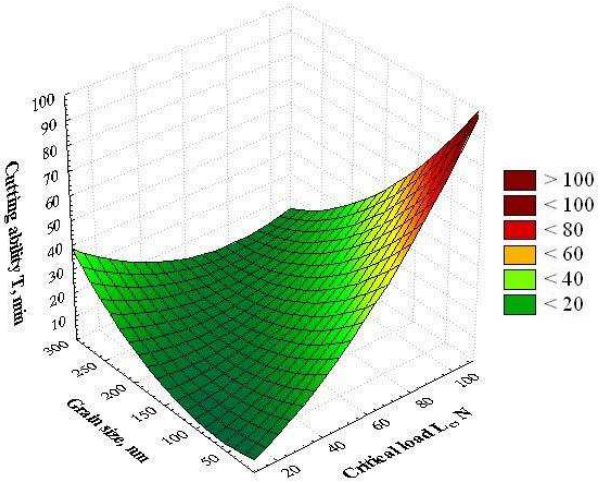

Figure 42. *Evaluation of the PVD and CVD coatings particle size and the critical load influence of tool life T for sialon ceramics tools coated with PVD and CVD coatings determined by artificial neural networks with a fixed thickness of 3.0 microns and coating microhardness 3600 HV0.05*

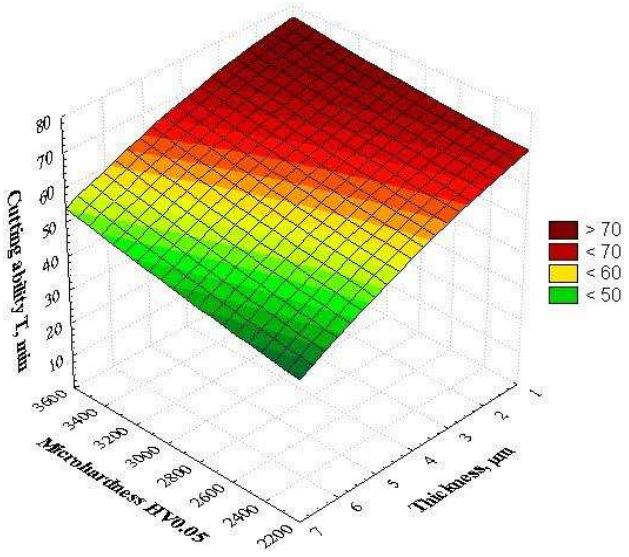

Figure 43. *Evaluation of the PVD and CVD coatings microhardness and the thickness influence of tool life T for sialon ceramics tools coated with PVD and CVD coatings determined by artificial neural networks with a fixed critical load L_c = 105 N and particle size 8.2 nm*

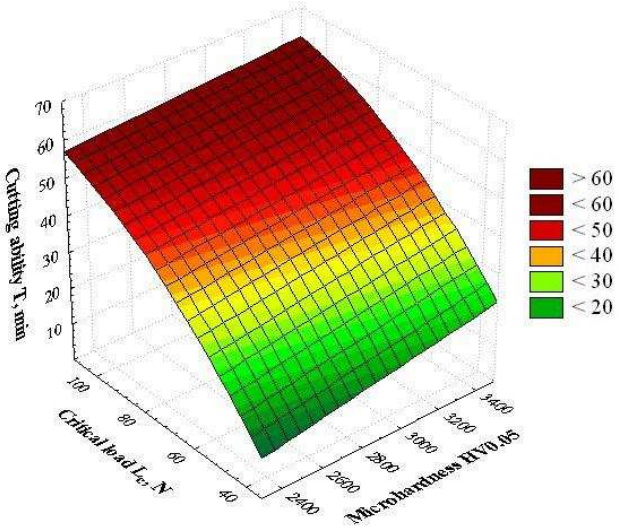

Figure 44. *Evaluation of the PVD and CVD coatings critical load and the microhardness influence of tool life T for sintered carbide tools coated with PVD and CVD coatings determined by artificial neural networks at a fixed coating thickness 2.5 microns and particle size 9.8 nm*

5. Summary

Production technologies and the application of surface layers have a stable position and are regarded as basic knowledge in the field of material engineering. A lot of research centers worldwide working on surface engineering are applying all possible means to fathom and describe the phenomena taking place on the surface of solids. Such a situation instigates scientists to undertake challenging research work aiming to increase the operating durability of surface layers, and, in consequence, the durability of the product [5,6]. The coatings resistant to wear have been successfully applied for around half a century, mainly on machining cutting edges from tooling steel and sintered carbides [7,43,53,81]. What is more, in spite of opinions that the coating of tooling ceramics is aimless due to its sufficiently enough hardness, we can observe an increasing interest in such solutions. A lot of research works [11,12] including also those carried out at the Division of Material Processing Technology, Management and Computer Techniques in Material Science of the Institute of Engineering Materials and Biomaterials of the Silesian University of Technology in Gliwice have been devoted to the problem of coating of tooling materials, including also the coating of tooling ceramics [1,14-29,42,45,52,65,72,73,75,86]. The research studies show that the deposition of thin coatings on the ceramic machining cutting edges is fully grounded, since it has been demonstrated that there is a rise of cutting abilities of ceramic tools covered by the coatings obtained in the PVD and CVD processes. It has been demonstrated that the deposition of coatings on the surface of machining tools such as sintered carbides, tooling cermets, ceramics on the basis of Al_2O_3 and Si_3N_4 contributes among others to a magnificent (around a dozen) rise of the durability of the cutting edge by lowering the wear of cutting edges as compared to the non-covered tools, to the improvement of tribological contact conditions in the contact area tool-machined object and to the protection of the cutting edge against oxidation and excessive heating. These effects directly contribute to the reduction of energy consumption during machining processes, they ensure appropriate technological reliability and reduce standstill incidents of the whole production lines resulting from insufficient durability of the tools.

The designing process of the system coating-cutting edge implies an appropriate selection of coating material in order to reduce or totally eliminate the dominating mechanism of cutting edge wear [55]. As it has been confirmed by numerous research studies, the coating should satisfy various requirements to ensure a suitable protection of the tool during the machining process. Literature studies show that the most important coating properties determining its operating qualities are undoubtedly hardness, adhesion to the substrate and grain size.

Therefore in the paper we present the results of research studies estimating the influence of coating properties on the durability of coated cutting edges.

In order to estimate the relation between the coating properties and operating durability of coated cutting edges we selected the following coatings of the PVD type: Ti(B,N), (Ti,Zr)N, Ti(C,N), Ti(C,N)+(Ti,Al)N, (Al,Ti)N, (Ti,Al)N, (Al,Cr)N and CVD coatings of the type Ti(C,N)+Al_2O_3+TiN and Ti(C,N)+TiN obtained on the substrates from sintered carbides and sialon ceramics. In there investigated coatings we applied solid solutions secondary isomorphic with titanium nitride TiN as well as chromium nitride CrN and aluminum oxide Al_2O_3 in the case of CVD coating.

Basing on the experimental results involving the operating durability we elaborated dependence models between the properties of the coatings and operating durability of the cutting edges covered by the investigated coatings using artificial neural networks. In effect of the carried out simulations it has been demonstrated that the change of coating adhesion to the substrate has most significant influence on the durability of machining cutting edges. Grain size, thickness and microhardness of the obtained coatings have lower influence than adhesion on the durability of cutting edges from sintered carbides and sialon ceramics since the change of these quantities has smaller impact of the operating durability T. However, it has been demonstrated that in congruence with the assumptions the durability of the cutting edge rises with the decreasing grain size, which is confirmed by literature studies [69,91,92,93]. The change of microhardness within the range from 2230 to 3600 HV0.05 has only slight influence on the improvement of cutting edge durability, which is confirmed by 3D images being the results of the simulation with the use of artificial neural networks. The elaborated durability models of the cutting edge can be useful for the prediction of operating properties in view of the knowledge on coating properties, without the necessity to carry out expensive and time consuming cutting ability trials.

Furthermore, in the case of coatings containing AlN phase of the hexagonal lattice, there occur covalence bonds analogous to those in ceramic substrate, which in effect yields good adhesion of these coatings to the substrate. It means that the type of interatomic bonds present in the material of substrate and coating has a great influence on the adhesion of the coatings to the substrate. It can be extremely helpful when selecting the coating material on ceramic cutting edges since the deposition of coatings on cutting edges in PVD processes is difficult due to their dielectric properties, because without the possibility to polarize the substrate during the deposition process it is difficult to obtain coatings which would have good adhesion to ceramic substrates.

Acknowledgements

The paper has been realised in relation to the project POIG.01.01.01-00-023/08 entitled "Foresight of surface properties formation leading technologies of engineering materials and biomaterials" FORSURF, co-founded by the European Union from financial resources of European Regional Development Found and headed by Prof. L.A. Dobrzański.

References

1. M. Adamiak, The structure and properties of TiN and Ti(C,N) coatings deposited in the PVD process on high speed steel. PhD thesis, Silesian University of Technology Library, Gliwice, 1997 (in Polish).
2. M. Arndt, T. Kacsich, Performance of new AlTiN coatings in dry and high speed cutting, Surface and Coatings Technology 163-164 (2003) 674-680.
3. M. Betiuk, T. Borowski, K. Burdyński, The (Ti,Al)N, (Ti,Al)C and (Ti,Al)CN multicompound coatings synthesis in low pressure of DC arc discharge, Engineering Materials 6 (2008) 674-678 (in Polish).
4. T. Burakowski, T. Wierzchoń, Engineering of metal surface, WNT, Warszawa 1995 (in Polish).
5. T. Burakowski, Transformation of superficial layers of areological system, Engineering Materials 6 (2008) 543-547 (in Polish).
6. T. Burakowski, Possibility of areology, Engineering Materials 5 (2006) 890-897 (in Polish).
7. S.I. Cha, S.H. Hong, B.K. Kim, Spark plasma sintering behavior of nanocrystalline WC-10Co cemented carbides powders, Materials Science & Engineering A351 (2003) 31-38.
8. Yin-Yu Chang, Da-Yung Wang, Characterization of nanocrystalline AlTiN coatings synthesized by a cathodic-arc deposition process, Surface and Coatings Technology 201 (2007) 6699-6701.
9. P. Cichosz, Cutting tools, WNT, Warszawa, 2006 (in Polish).
10. F. Čuš, M. Soković, J. Kopač, J. Balič, Model of complex optimization of cutting conditions. Journal of Materials Processing Technology 64 (1997) 41-52.
11. K. Czechowski, I. Pofelska-Filip, P. Szlosek, A. Fedaczyński, J. Kasina, B. Królicka, Chosen properties of hard layers deposited on ceramic material cutting inserts and their influence on the inserts durability, Engineering Materials 5 (2005) 261-264 (in Polish).
12. K. Czechowski, I. Pofelska-Filip, P. Szlosek, B. Królicka, J. Wszołek, Forming the functional properties of cutting inserts of composite oxide-carbide ceramics by nanostructural coatings deposited using the arc PVD method, Engineering Materials 5 (2006) 913-916 (in Polish).

13. D-Y. Wang, C-L. Chang, C-H. Hsu, H-N. Lin, Synthesis of (Ti,Zr)N hard coatings by unbalanced magnetron sputtering, Surface and Coatings Technology 130 (2000) 64-68.
14. L.A. Dobrzański, M. Adamiak, G.E. D'Errico, Relationship between erosion resistance and the phase and chemical composition of PVD coatings deposited onto high-speed steel, Journal of Materials Processing Technology 92-93 (1999) 184-189.
15. L.A. Dobrzański, M. Adamiak, Structure and properties of the TiN and Ti(C,N) coatings deposited in the PVD process on high-speed steels, Journal of Materials Processing Technology 133 (2003) 50-62.
16. L.A. Dobrzański, K. Gołombek, E. Hajduczek, Structure of the nanocrystalline coatings obtained on the CAE process on the sintered tool materials, Journal of Materials Processing Technology 175 (2006) 157-162.
17. L.A. Dobrzański, K. Gołombek, J. Kopač, M. Soković, Effect of depositing the hard surface coatings on properties of the selected cemented carbides and tool cermets, Journal of Materials Processing Technology 157-158 (2004) 304-311.
18. L.A. Dobrzański, K. Gołombek, J. Mikuła, D. Pakuła, Multilayer and gradient PVD coatings on the sintered tool materials, Journal of Achievements in Materials and Manufacturing Engineering 31/2 (2008) 170-190.
19. L.A. Dobrzański, K. Gołombek, Characteristic of nanocrystalline coatings obtained in cathode arc evaporation process onto sintered tool materials, Engineering Materials 3 (2006) 368-371 (in Polish).
20. L.A. Dobrzański, K. Gołombek, Gradient coatings deposited by Cathodic Arc Evaporation: characteristic of structure and properties, Journal of Achievements in Materials and Manufacturing Engineering 14/1-2 (2006) 48-53.
21. L.A. Dobrzański, K. Gołombek, Structure and properties of the cutting tools made from cemented carbides and cermets with the TiN + mono-, gradient- or multi (Ti,Al,Si)N+TiN nanocrystalline coatings, Journal of Materials Processing Technology 164-165 (2005) 805-815.
22. L.A. Dobrzański, J. Mikuła, Structure and properties of PVD and CVD coated Al_2O_3+TiC mixed oxide tool ceramics for dry on high speed cutting processes, Journal of Materials Processing Technology 164-165 (2005) 822-831.
23. L.A. Dobrzański, J. Mikuła, The structure and functional properties of PVD and CVD coated Al_2O_3+ZrO_2 oxide tool ceramics, Journal of Materials Processing Technology 167 (2005) 438-446.
24. L.A. Dobrzański, D. Pakuła, E. Hajduczek, Structure and properties of the multi-component TiAlSiN coatings obtained in the PVD process in the nitride tool ceramics, Journal of Materials Processing Technology 157-158 (2004) 331-340.
25. L.A. Dobrzański, D. Pakuła, A. Křiž, M. Soković, J. Kopač, Tribological properties of the PVD and CVD coatings deposited onto the nitride tool ceramics, Journal of Materials Processing Technology 175 (2006) 179-185.
26. L.A. Dobrzański, M. Polok, M. Adamiak, Structure and properties of PVD coatings on tool steel for nitriding X37CrMoV5-1 to hot work steel, Proceedings of the Third Scientific Conference M^3E'2005, Gliwice–Wisła 2005, 159-166 (in Polish).

27. L.A. Dobrzański, M. Staszuk, J. Konieczny, W. Kwaśny, M. Pawlyta, Structure of TiBN coatings deposited onto cemented carbides and sialon tool ceramics, Archives of Materials Science and Engineering 38/1 (2009) 48-54.
28. L.A. Dobrzański, M. Staszuk, J. Konieczny, J. Lelątko, Structure of gradient coatings deposited by CAE-PVD techniques, Journal of Achievements in Materials and Manufacturing Engineering 24/2 (2007) 55-58.
29. L.A. Dobrzański, M. Staszuk, M. Pawlyta, W. Kwaśny, M. Pancielejko, Characteristics of Ti(C,N) and (Ti,Zr)N gradient PVD coatings deposited onto sintered tool materials, Journal of Achievements in Materials and Manufacturing Engineering 31/2 (2008) 629-634.
30. L.A. Dobrzański, Forming the structure and surface properties of engineering and biomedical materials, Foresight of surface properties formation leading technologies of engineering materials and biomaterials, International OCSCO World Press, Gliwice, 2009. (in Polish)
31. L.A. Dobrzański, The modern tendency into range of development sintered tool materials, Mechanics 1 (1987) 21-31. (in Polish)
32. L.A. Dobrzański, Design and manufacturing functional gradient tool materials - dependence properties on technology and thickness of surface layers with a gradient of both chemical and phase composition manufactured on tool from different applications. Design and manufacturing functional gradient materials, The Polish Academy of Science, Cracow, 2007 (in Polish).
33. S. Dolinšek, J. Kopač, Acoustic emission signals for tool wear identification, Wear 225-229 (1999) 295-303.
34. S. Dolinšek, J. Kopač, Mechanism and types of tool wear; particularities in advanced cutting materials, Journal of Achievements in Materials and Manufacturing Engineering 19/1 (2006) 11-18.
35. Z. Dongli, Y. Dianran, X. Lisong, D. Yanchun, Characterization of nanostructured TiN coatings fabricated by reactive plasma spraying, Surface & Coatings Technology 202 (2008) 1928-1934.
36. L.A. Donohue, J. Cawley, J.S. Brooks, Deposition and characterization of arc-bond sputter Ti_xZr_yN coatings from pure metallic and segmented targets, Surface and Coatings Technology 72 (1995) 128-138.
37. I. Dörfel, W. Österle, I. Urban, E. Bouzy, Microstructural characterization of binary and ternary hard coating systems for wear protection. Part I: PVD coatings, Surface and Coatings Technology 111/2-3 (1999) 199-209.
38. J.L. Endrino, V.H. Derflinger, The influence of alloying elements on the phase stability and mechanical properties of AlCrN coatings, Surface & Coatings Technology 200 (2005) 988-992.
39. G.S. Fox-Rabinovich, J.L. Endrino, B.D. Beake, A.I. Kovalev, S.C. Veldhuis, L. Ning, F. Fontaine, A. Gray, Impact of annealing on microstructure, properties and cutting performance of an AlTiN coating, Surface and Coatings Technology 201 (2006) 3524-3529.
40. C. Gautier, H. Moussaoui, F. Elstner, J. Machet, Comparative study of mechanical and structural properties of CrN films deposited by d.c. magnetron sputtering and vacuum arc evaporation, Surface & Coatings Technology 86-87/1 (1996) 254-262.
41. W. Gissler, P.N. Gibson, Titanium implantation into born nitride films and ion-beam mixing of titanium born nitride multilayers, Ceramics International 22 (1996) 335-340.

42. K. Gołombek: The structure and properties of sintered carbides and cermets tool coated in PVD process by anti-wear coatings. PhD Thesis, Silesian University of Technology Library, Gliwice 2001 (in Polish)
43. J.R. Groza, A. Zavaliangos, Sintering activation by external electrical field, Materials Science & Engineerin A 287 (2000) 171-177.
44. W. Grzesik, Z. Zalisz, S. Król, Tribological behaviour of TiAlN coated carbides in dry sliding tests, Journal of Achievements in Materials and Manufacturing Engineering 17/1-2 (2006) 181-184.
45. H. Hahn, P. Mondal, K.A. Padmanabhan, Nanostructured Materials 9 (1997) 603.
46. S. Hampshire, Silicon nitride ceramics - review of structure, processing and properties. Journal of Achievements in Materials and Manufacturing Engineering 24/1 (2007) 43-50.
47. Y. He, I. Apachitei, J. Jhou, W. Walstock, J. Duszczyk, Effect of prior plasma nitriding applied to a hot-work tool steel on the scratch-resistant properties of PACVD TiBN and TiCN coatings, Surface & Coatings Technology 201 (2006) 2534-2539.
48. P. Holubar, M. Jilek, M. Sima, Nanocomposite nc-TiAlSiN and nc-TiN–BN coatings: their applications on substrates made of cemented carbide and results of cutting tests, Surface and Coatings Technology 120-121 (1999) 184-188.
49. P. Holubar, M. Jilek, M. Sima, Present and possible future applications of superhard nanocomposite coatings, Surface and Coatings Technology 133-134 (2000) 145-151.
50. H. Holzschuh, Deposition Ti-B-N (single and multilayer) and Zr-B-N coatings by chemical vapor deposition techniques on cutting tools, Thin Solid Films 469-470 (2004) 92-98.
51. S. Jonsson, Trita-Mac 506, The Royal Institute of Technology, Div. Physical Mettalurgy, Stockholm, 1992.
52. A. Kloc-Ptaszna: Structure and properties of gradient carbide steel sintered onto groundmass of HS6-5-2 high speed steel. PhD Thesis, Silesian University of Technology Library, Gliwice, 2007 (in Polish).
53. J. Kopač, M. Soković, S. Dolinšek, Tribology of coated tool in conventional and HSC machining, Journal of Materials Processing Technology 118 (2001) 377-384.
54. J. Kopač, Influence of cutting material and coating on tool quality and tool life, Journal of Materials Processing Technology 78 (1998) 95-103.
55. M. Kupczyk, Identification of damage and loss adherence were resistance coatings to edges machineable in adhesion test. Archive of Machine Technology and Automation 21/2 (2001) 231-251 (in Polish).
56. M. Kupczyk, Surface engineering. Wear resistant coatings for cutting edges, Poznań University of Technology Publishing House, Poznań, 2004 (in Polish).
57. T. Kurita, M. Hattori, Development of new-concept desk top size machine tool, International Journal of Machine Tools & Manufacture 45 (2005) 959-965.
58. W. Kwaśny, The structure and properties of coatings obtained in PVD process on sintered high speed steel. PhD Thesis, Silesian University of Technology Library, Gliwice, 2001 (in Polish).

59. T. Leyendecker, O. Lammer, S. Esser, J. Ebberink, The development of the PVD coating TiAlN as a commercial coating for cutting tools, Surface and Coatings Technology 49 (1991) 175-178.
60. Y.H. Lu, Z.F. Zhou, P. Sit, Y.G. Shen, K.Y. Li, Haydn Chen, X-Ray photoelectron spectroscopy characterization of reactively sputtered Ti–B–N thin films, Surface & Coatings Technology 187 (2004) 98-105.
61. K. Lukaszkowicz: Structure and properties of wear resistance and corrosion resistant PVD multilayer coatings. PhD Thesis, Silesian University of Technology Library, Gliwice 2001. (in Polish)
62. A. Michalski, Physical chemistry bases obtaining coatings from gas phase. Outhosue Publishing of Warsaw Technical University Oficyna, Warsaw 2000 (in Polish).
63. A. Michalski, PVD methods applied to deposition both hard and low-fusible material layers on machining tools, Metal science, Heat treatment 79 (1986) 18-23 (in Polish).
64. M. Michalski, D. Siemaszko, Impulsive plasma sintering of WC-12Co nanocrystalline carbides. Engineering materials 3 (2006) 629-631 (in Polish).
65. J. Mikuła, Structure and properties oxides tool ceramic on Al_2O_3 base from PVD and CVD wear resistance coatings. PhD Thesis, Silesian University of Technology Library, Gliwice, 2004 (in Polish).
66. C. Mitterer, P. Losbichler, F. Hofer, P. Warbichler, P.N. Gibson, W. Gissler, Nanocrystalline hard coatings within the quasi-binary system TiN-TiB_2, Vacuum 50 (1998) 313-318.
67. T.P. Mollart, J. Haupt, R. Gilmore, W. Gissler, Tribological behaviour of homogeneous Ti-B-N, Ti-B-N-C and TiN/h-BN/TiB_2 multilayer coatings, Surface and Coatings Technology 86-87 (1996) 231-236.
68. B.A. Movchan, K.Yu Yakovchuk, Graded thermal barrier coatings, deposited by EB-PVD, Surface and Coatings Technology 188-189 (2004) 85-92.
69. J. Musil, Hard and superhard nanocomposite coatings. Surface and Coatings Technology 125 (2000) 322-330.
70. B. Navinšek, P. Panjan, F. Gorenjak, Improvement of hot forging manufacturing with PVD and DUPLEX coatings, Surface and Coatings Technology 137 (2001) 255-264.
71. A.J. Novinrooz, H. Seyedi, M.M. Larijani, Microhardness study of Ti(C,N) films deposited on S-316 by the Hallow Cathode Discharge Gun, Journal of Achievements in Materials and Manufacturing Engineering 14/1-2 (2006) 59-63.
72. D. Pakuła, L.A. Dobrzański, K. Gołombek, M. Pancielejko, A. Kříž, Structure and properties of the Si_3N_4 nitride ceramics with hard wear resistant coatings, Journal of Materials Processing Technology 157-158 (2004) 388-393.
73. D. Pakuła, Structure and properties of PVD and CVD multilayer coatings resistant to abrasion on nitride ceramic tool Si_3N_4. PhD Thesis, Silesian University of Technology Library, Gliwice, 2003 (in Polish).
74. M. Pancielejko, W. Precht, Structure, chemical and phase composition of hard titanium carbon nitride coatings deposited on HS 6-5-2 steel, Journal of Materials Processing Technology 157-158 (2004) 394-298.

75. M. Polok, Structure and properties of PVD coatings deposited onto substrate from X37CrMoV5-1 steel heat treated and plasma nitride. PhD Thesis, Silesian University of Technology Library, Gliwice 2005 (in Polish).
76. W.M. Posadowski, Modern techniques of magnetron atomization, Electronics 4 (2006) 40-43 (in Polish).
77. W. Precht, E. Łunarska, A. Czyżniewski, Corrosion Resistance, Structure and Mechanical Properties of PVD, TiC_xN_{1-x} Coatings. Vacuum 47 (1996) 867-869.
78. W. Precht, Recent advances in hard and superhard anti-wear coating technology, Engineering Materials 3 (2006) 513-515 (in Polish).
79. L. Przybylski, Modern ceramic tool materials. Monograph 276, Technical University of Cracow, Cracow, 2000 (in Polish).
80. A.E. Reiter, V.H. Derflinger, B. Hanselmann, T. Bachmann, B. Sartory, Investigation of the properties of $Al_{1-x}Cr_xN$ coatings prepared by cathodic arc evaporation, Surface & Coatings Technology 200 (2005) 2114-2122.
81. S.H. Risbud, C-H. Shan, Fast consolidation of ceramic powders, Materials Science & Engineering A 204 (1995) 146-151.
82. H. Ronkainen, I. Nieminen, I. Holminen, K. Holmberg, A. Leyland, A. Matthews, B. Matthes, E. Broszeit, Evaluation of some titanium-based ceramic coatings on high speed steel cutting tools, Surface and Coatings Technology 49 (1991) 468-473.
83. D.M. Sanders, Review ion-based coating processes derived from the cathodic arc, The Journal of Vacuum Science and Technology 7/3 (1989) 2339-2345.
84. M. Soković, M. Bahor, On the inter-relationships of some machinability parameters in finish machining with cermet TiN (PVD) coated tools, Journal of Materials Processing Technology 78/1-3 (1998) 163-170.
85. M. Soković, J. Mikuła, L.A. Dobrzański, J. Kopač, L. Koseč, P. Panjan, J. Madejski, A. Piech, Cutting properties of the $Al_2O_3 + SiC_{(w)}$ based tool ceramic reinforced with the PVD and CVD wear resistant coatings, Journal of Materials Processing Technology 164-165 (2005) 924-929.
86. M. Staszuk, The structure and properties of PVD and CVD gradient coatings deposited on sialons and sintered carbides. PhD Thesis, Silesian University of Technology Library, Gliwice, 2009 (in Polish).
87. S. Stolarz, High-melting compounds and phases. Publication of Silesia, Katowice 1974 (in Polish).
88. D.G. Teer, J. Hampshire, V. Fox, V. Bellido-Gonzalez, The tribological properties of MoS_2/metal composite coatings deposited by closed field magnetron sputtering, Surface and Coating Technology 94-95 (1997) 572-577.
89. J.A. Thornton, Journal of Vacuum Science and Technology A 4/6 (1986) 3059-3065.
90. V.V. Uglov, V.M. Anishchik, S.V. Zlotski, G. Abadias, The phase composition and stress development in ternary Ti-Zr-N coatings grown by vacuum arc with combining of plasma flows, Surface & Coatings Technology 200 (2006) 6389-6394.

91. S. Veprek, A.S. Argon, Towards the understanding of mechanical properties of super- and ultrahard nanocomposites, Journal of Vacuum Science and Technology B 20 (2002) 650-664.
92. S. Veprek, S. Reiprich, A concept for the design of novel superhard coatings, Thin Solid Films 268 (1995) 64-71.
93. S. Veprek, New development in superhard coatings: The superhard nanocrystalline-amorphous composites, Thin Solid Films 317 (1998) 449-454.
94. B.G. Wendler, W. Pawlak, Low friction and wear resistant coating systems on Ti6Al4V alloy, Journal of Achievements in Materials and Manufacturing Engineering 26/2 (2008) 207-210.
95. Z. Werner, J. Stanisławski, J. Piekoszewski, E.A. Levashov, W. Szymczyk, New types of multi-component hard coatings deposited by ARC PVD on steel pre-treated by pulsed plasma beams, Vacuum 70 (2003) 263-267.
96. M. Wysiecki, Contemporary Tool Materials, WNT, Warszawa, 1997 (in Polish).

The paper is published also in the Journal of Achievements in Materials and Manufacturing Engineering